

1 **A Central Asia Hydrologic Monitoring Dataset for Food and**
2 **Water Security Applications in Afghanistan**

3 Amy L. McNally^{1,2,3}, Jossy Jacob^{1,4}, Kristi Arsenault^{1,2}, Kimberly Slinski^{1,5}, Daniel P. Sarmiento^{1,2},
4 Andrew Hoell⁶, Shahriar Pervez⁷, James Rowland⁸, Mike Budde⁸, Sujay Kumar¹, Christa Peters-
5 Lidard¹, James P. Verdin³

6

7 1 NASA Goddard Space Flight Center, Greenbelt, MD, 20771, United States

8 2 Science Applications International Corporation Inc., Reston, VA, 20190, United States

9 3 U.S. Agency for International Development, Washington, DC, 20523, United States

10 4 Science Systems and Applications Inc., Lanham, MD, 20706, United States

11 5 University of Maryland Earth Systems Science Interdisciplinary Center, College Park, MD,
12 20740, United States

13 6 National Oceanic and Atmospheric Administration, Physical Science Laboratory, Boulder, CO,
14 80305, United States

15 7 Arctic Slope Regional Corporation Federal Data Solutions, Contractor to U.S. Geological Survey,
16 Earth Resources Observation and Science (EROS) Center, Sioux Falls, SD, 57198, United States

17 8 U.S. Geological Survey, EROS Center, Sioux Falls, South Dakota, 57198, United States

18

19 *Correspondence to:* Amy L. McNally (amy.l.mcnally@nasa.gov)

20 **Abstract**

21
22 From the Hindu Kush Mountains to the Registan desert, Afghanistan is a diverse landscape where
23 droughts, floods, conflict, and economic market accessibility pose challenges for agricultural
24 livelihoods and food security. The ability to remotely monitor environmental conditions is critical to
25 support decision making for humanitarian assistance. The Famine Early Warning Systems Network
26 (FEWS NET) Land Data Assimilation System (FLDAS) global and Central Asia data streams
27 provide information on hydrologic states for routine integrated food security analysis. While
28 developed for a specific project, these data are publicly available and useful for other applications
29 that require hydrologic estimates of the water and energy balance. These two data streams are
30 unique because of their suitability for routine monitoring, as well as a historical record for
31 computing relative indicators of water availability. The global stream is available at ~1 month
32 latency, monthly average outputs on a 10-km grid from 1982-present. The second data stream,
33 Central Asia (30-100 °E, 21-56 °N), at ~1 day latency, provides daily average outputs on a 1-km
34 grid from 2000-present. This paper describes the configuration of the two FLDAS data streams,
35 background on the software modeling framework, selected meteorological inputs and parameters,
36 and results from previous evaluation studies. We also provide additional analysis of precipitation
37 and snow cover over Afghanistan. We conclude with an example of how these data are used in
38 integrated food security analysis. These data are hosted by the National Aeronautics and Space
39 Administration (NASA) and U.S. Geological Survey data portals for use in new and innovative
40 studies that will improve understanding of this region.

41 **1 Introduction**

42 From the Hindu Kush Mountains to the Registan desert, Afghanistan is a diverse landscape where
43 droughts, floods, conflict, and economic market accessibility pose challenges for agricultural
44 livelihoods and food security. The ability to remotely monitor environmental conditions is critical to
45 support decision making for economic development, humanitarian assistance, water resource
46 management, agriculture and more. Environmental datasets can be combined with socio-economic
47 variables and transformed into customized products to support decision making. This is the
48 definition of a ‘climate service’ (Hewitt et al., 2012).

49
50 Hydrologic and land surface datasets are particularly relevant for agriculture and water resources
51 decision making. When these datasets are credible, updated routinely, and made publicly available,
52 the influences of climate variability and climate change can be incorporated into specialized
53 analyses by intermediary users¹. One example of an intermediary user central to this data descriptor
54 is the food security analysts of the Famine Early Warning Systems Network (FEWS NET). FEWS
55 NET analysts combine environmental information, largely from remote sensing and earth system
56 models, with information on nutrition, livelihoods, markets, and trade to provide decision support to

¹ The WMO defines intermediate (intermediary) users as those who transform climate information into a climate service

57 the U.S. Agency for International Development (USAID) Bureau of Humanitarian Assistance.
58 Additional examples and discussion of the production of climate service inputs can be found in the
59 literature (e.g., Vincent et al., 2018; McNally et al., 2019).
60

61 While these data are tailored to specific needs, they are also applicable to other climate services and
62 research e.g., Desert Locusts movement forecasting (Tabar et al., 2021). To that end, this paper
63 describes the FEWS NET Land Data Assimilation System (FLDAS) global and Central Asia data
64 streams. The inputs (e.g., precipitation) and resulting hydrologic estimates (a) provide a 40+ year
65 historical record for contextualizing estimates in terms of departures from average (i.e., anomalies),
66 (b) are low latency (< 1-month) for timely decision support, and (c) are familiar to the food and
67 water security user-community.

68
69 The purpose of this data descriptor is four-fold:

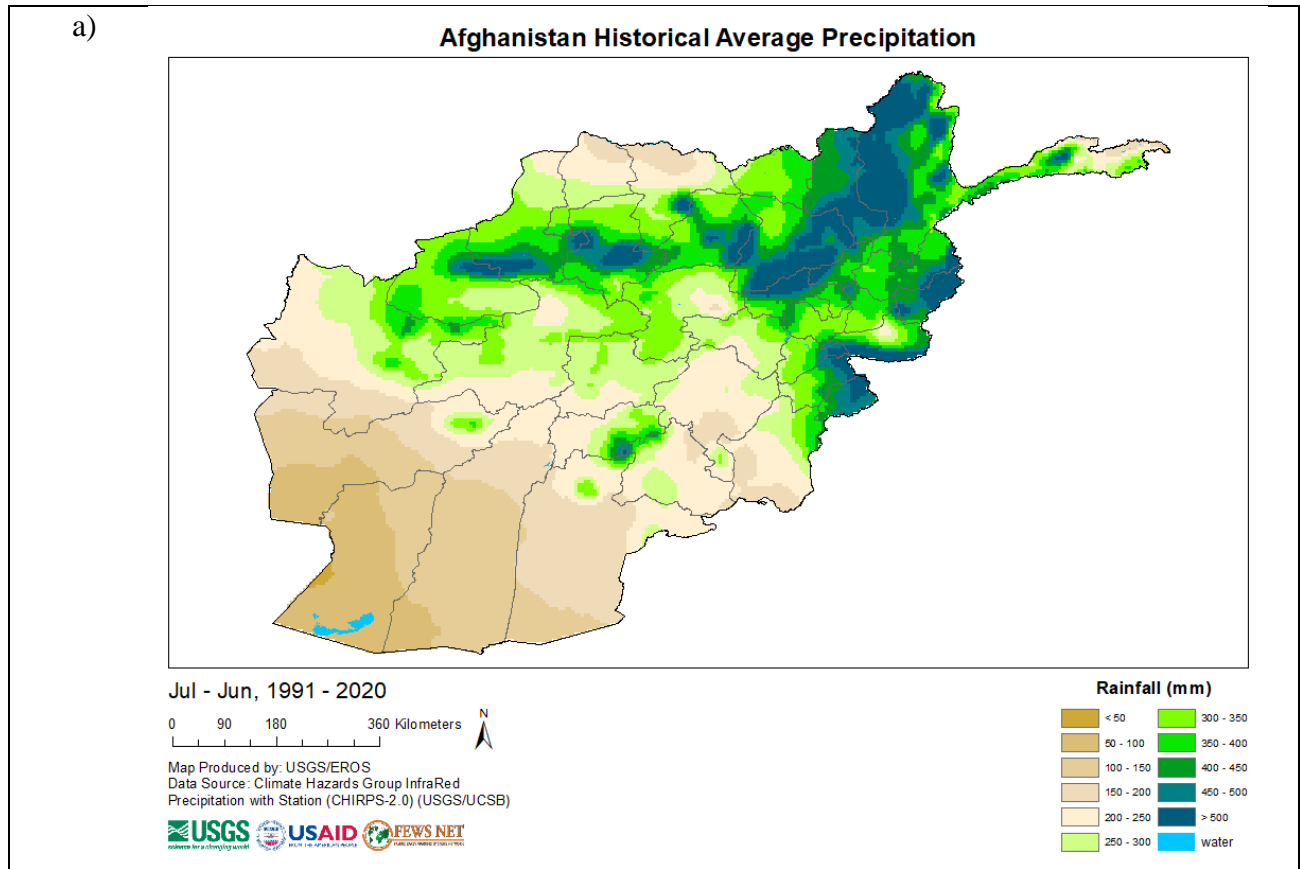
- 70 • to describe the development of the moderate resolution, low latency FLDAS hydrologic
71 monitoring system for Central Asia, specifically Afghanistan
- 72 • to increase awareness of these data resources, which are intended to be a public good,
- 73 • to demonstrate how our methods inform critical investigations that ultimately improve
74 general understanding of water resources in this important region of the world, and
- 75 • to describe a ‘convergence of evidence’ approach to hydrologic monitoring in locations
76 where all sources of information contain some level of uncertainty.
77

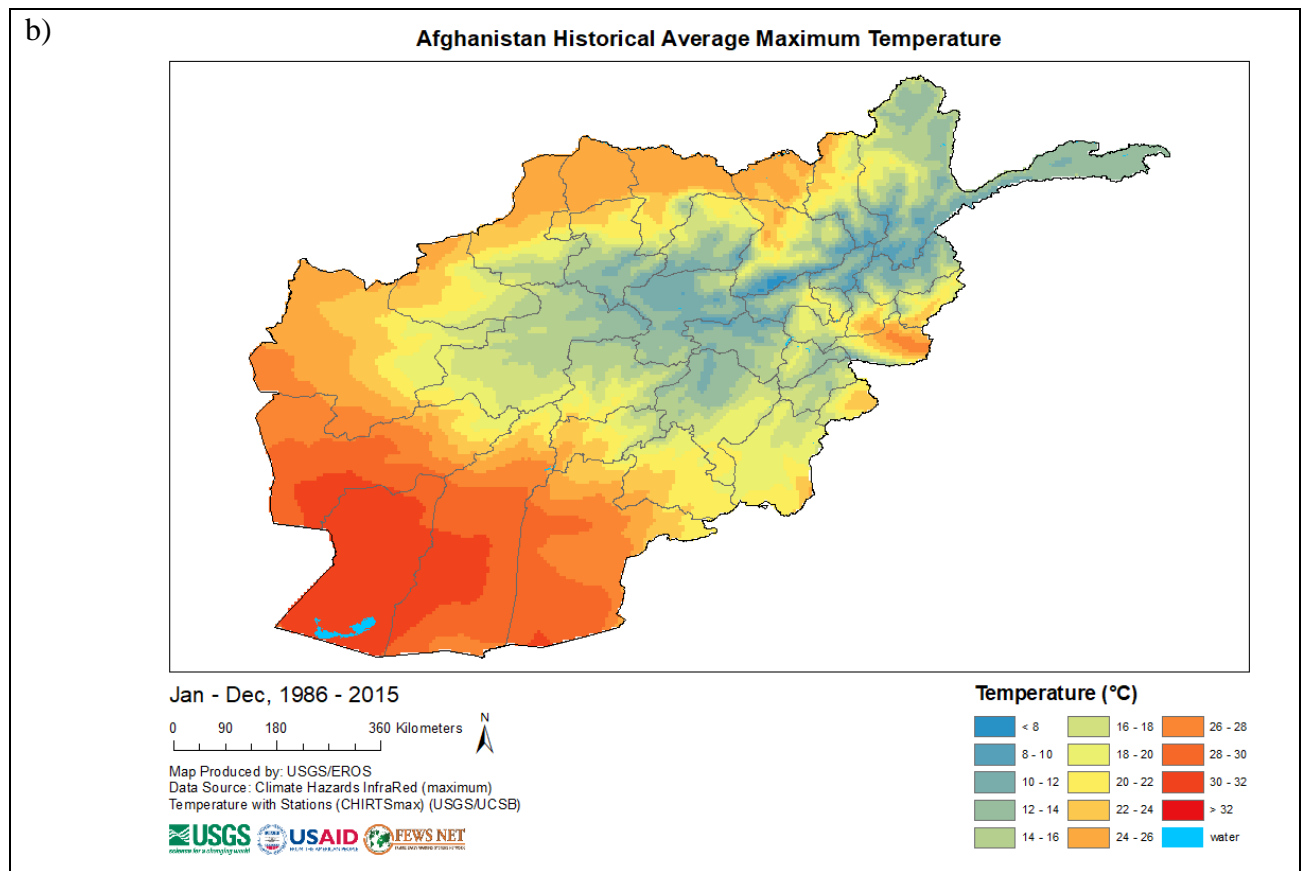
78 An outline of this data descriptor is as follows. Section 1.1 provides background on Afghanistan
79 Weather and Climate. Section 1.2 reviews previous studies that have conducted evaluations of the
80 meteorological inputs and hydrologic outputs of Land Data Assimilation Systems in the Central
81 Asia region. Section 2 (Methods) describes the hydrologic modeling system, parameters and
82 meteorological inputs, and model outputs. Section 3 (Results) presents comparisons of precipitation
83 inputs, and comparisons of modeled snow estimates to remotely sensed snow observations. Finally,
84 Section 4 describes an application of these data to the Afghanistan drought of 2018.

85 **1.1 Afghanistan Weather and Climate**

86 Central Asia, a region that includes Afghanistan, is water-scarce, receiving roughly 75% of its
87 annual precipitation during November–April (Oki and Kanae, 2006). In Afghanistan, rainfall is
88 highest in the northeast Hindu Kush Mountains and decreases toward the arid southwest Registan
89 Desert (Fig. 1a). Temperature follows a similar pattern with cooler temperatures in the high
90 elevation, wetter northeast and warmer temperatures in the south and southwest (Fig. 1b). Regional
91 precipitation is strongly influenced by the El Niño-Southern Oscillation (ENSO). La Niña
92 conditions are associated with below average precipitation (FEWS NET, 2020b) and El Niño
93 conditions are associated with above average precipitation (Barlow et al., 2016; Hoell et al., 2017;
94 Rana et al., 2018; Hoell et al., 2018, 2020; FEWS NET, 2020a). Other factors with an important
95 influence on precipitation include orography, storm tracks, and the Madden–Julian oscillation
96 (Barlow et al., 2005; Nazemosadat and Ghaedamini, 2010; Hoell et al., 2018). The last several years

97 have experienced several ENSO events, with recent La Niña events in 2016-17, 2017-18, and 2020-
98 2022 (NOAA CPC ENSO Cold & Warm Episodes by Season, 2021) that corresponded to droughts
99 (FEWS NET, 2017b, 2018c, 2021).
100





101 Figure 1. (a) Average annual precipitation in Afghanistan from 1991-2020, with overlaid province
 102 boundaries. (b) Average maximum monthly temperature from (1986-2015), overlaid with province
 103 boundaries. Map source (USGS Knowledge Base, 2021).

104
 105 Despite Afghanistan’s semi-arid climate, agriculture is an important sector, contributing 23% of its
 106 gross domestic product and employing 44% of the national labor force (CIA World Factbook). High
 107 mountain snowpack and snowmelt runoff are important for agricultural water supply. According to
 108 FEWS NET (2018b) snowmelt runoff is responsible for “providing over 80% of irrigation water
 109 used. The timing and duration of the snowmelt is a key factor in determining the volume of
 110 irrigation water and the length of time that it is available, as well as its availability for use in
 111 marginal areas that experience [variable] rainfall.” Therefore, routine hydrologic monitoring, with a
 112 particular emphasis on snow, is critical for tracking agricultural conditions and provides early
 113 warning for food insecurity.

114 1.2 Hydrologic Data Availability and Uncertainty

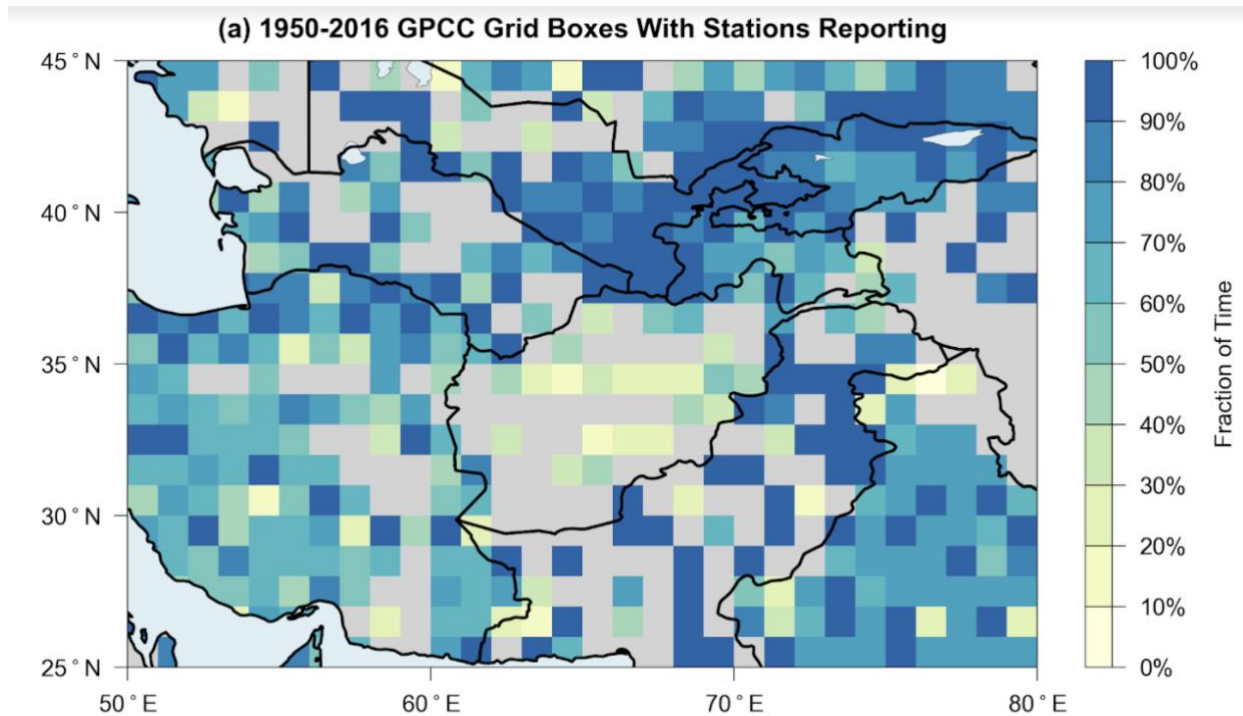
115 Remote sensing and models are important inputs to climate services (Qamer et al., 2019). In the
 116 Central Asia region, and especially Afghanistan estimates of meteorological inputs, and model
 117 parameters have considerable uncertainty due to sparse in situ environmental observations. To

118 address these challenges, the NASA High Mountain Asia project (<https://www.himat.org/>) has
119 broadly aimed to explore the driving changes in hydrology as well as model validation and data
120 assimilation, and water budget processes from the Himalayas in the south and east to the Hindu
121 Kush in the west. These efforts and other studies of satellite derived rainfall informed the
122 configuration and interpretation of the FLDAS Central Asia and global data streams.

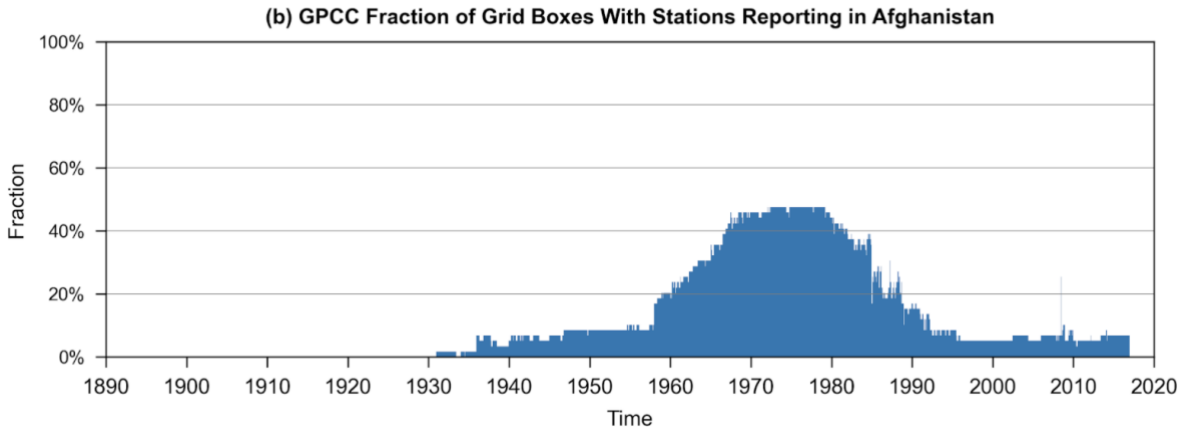
123

124 The primary challenge to producing and evaluating hydrologic estimates is that sparse in situ
125 precipitation observations lead to uncertainty in gridded, satellite-based precipitation estimates.
126 Precipitation station observations are used for (a) bias correction of satellite estimates and (b)
127 validation of gridded products. In terms of gridded dataset development, Hoell et al. (2015) describe
128 how lack of station observations and complex topography in Afghanistan, Iraq, and Pakistan makes
129 this issue particularly problematic. Barlow et al. (2016) also highlight the station availability across
130 the region and how that influences uncertainties in the Global Precipitation Climatology Center
131 (GPCC) version 6 (Schneider et al., 2017) dataset over Central Asia (Fig. 2a) and specifically
132 Afghanistan over time (Fig. 2b).

133



134



135
 136 Figure 2. (a) Station data availability underlying the GPCC version 6 dataset, for the 1950–2016
 137 period, on the 0.5°-resolution grid over Central Asia. (b) Fraction of gridcells with Number of
 138 stations used as input to the GPCC rainfall dataset in Afghanistan from 1932-2016.
 139

140 In the absence of abundant in situ observations, one approach for remote sensing and model
 141 evaluation is to compare multiple input datasets and evaluate the water balance. Independent
 142 observations from the different components of the water balance (e.g., evapotranspiration, soil
 143 moisture, streamflow) help constrain estimates. We provide some background here and refer readers
 144 and data users to literature from the NASA High Mountain Asia project, specifically Yoon et al.
 145 (2019) and Ghatak et al. (2018), who explored similar configurations to the FLDAS system. This
 146 background allows the reader to appreciate the uncertainties in inputs, outputs and derived products
 147 and climate services over Afghanistan and the broader Central Asia region.
 148

149 Meteorological forcing is known to be the primary source of uncertainty in land surface model
 150 simulations (Kato and Rodell, 2007). Thus, its evaluation is important to understand the quality of
 151 model inputs and outputs. For this reason, Ghatak et al. (2018) compare four unique precipitation
 152 data sources: daily Climate Hazards center Infrared Precipitation with Stations (CHIRPS) (Funk et
 153 al., 2015), NOAA’s Global Data Assimilation System (GDAS) (Derber et al., 1991), and two
 154 estimates from NASA’s Modern Era Reanalysis for Research and Applications version 2 (MERRA-
 155 2) (Gelaro et al., 2017). They find that annual CHIRPS and GDAS precipitation estimates had
 156 similar bias and root mean squared error over Afghanistan with respect to APHRODITE (Asian
 157 Precipitation Highly Resolved Observational Data Integration Toward Evaluation) rain-gauge
 158 derived product (Yatagai et al., 2012). CHIRPS had a higher correlation with APHRODITE. Ghatak
 159 et al. (2018) further evaluated the quality of rainfall inputs based on the performance of
 160 evapotranspiration and other derived outputs. The authors caution that gridded precipitation
 161 estimates that have in situ inputs, like CHIRPS, may systematically underestimate precipitation in
 162 mountainous regions. We keep this consideration in mind when interpreting differences between
 163 FLDAS global and Central Asia data streams.
 164

165 Yoon et al. (2019) compare precipitation estimates from 10 different products including
166 APHRODITE, CHIRPS, GDAS, and MERRA-2, across a broad region of High Asia, including a
167 portion of Afghanistan. They find that all datasets generally capture the spatial pattern of rainfall
168 and that the products tend to agree more at high elevations, where it is unlikely there are station
169 observations. Like Ghatak et al. (2018), they found CHIRPS and APHRODITE to have a lower
170 average precipitation than GDAS, attributable to the incorporation of sparse gauge data.

171
172 In addition to precipitation, other meteorological inputs are important for accurate hydrologic
173 estimates. Yoon et al. (2019) conducted an intercomparison of near surface air temperature
174 estimates from three model analysis products (European Centre for Medium-Range Weather
175 Forecasts (ECMWF; Molteni et al., 1996), GDAS, and MERRA-2). They noted a statistically
176 significant upward trends in GDAS and ECMWF temperature, as well as consistently higher
177 temperatures in MERRA-2. We see the same pattern when averaging across Afghanistan. Yoon et
178 al. (2019) conclude that improvements in the meteorological boundary conditions would be needed
179 to reduce the uncertainty in the terrestrial budget estimates. These sentiments are echoed in Qamer
180 et al. (2019).

181
182 Despite known uncertainties, Schiemann et al. (2008) find that gridded precipitation estimates can
183 qualitatively identify large scale spatial distribution of precipitation, seasonal cycles, and interannual
184 variability (i.e., wet and dry years) across Central Asia. Long-term estimates of rainfall from
185 satellite derived products, as well as derived historical time series from hydrologic modeling, can be
186 used as a baseline of “observations,” from which we can have a sense of relative conditions, i.e.,
187 anomalies and variability. When this historical record is harmonized with a routine monitoring
188 system, current conditions can be placed in historical context. Anomaly-based representation of
189 hydrologic extremes can provide confidence in modeled estimates that have the potential to
190 influence agricultural, water resources and food security outcomes. For these reasons one of the
191 requirements for FLDAS input is that there is a sufficiently long historical record for
192 contextualizing estimates in terms of anomalies.

193
194 From a climate services perspective, the reliance on the representation of relatively wet and dry
195 conditions, as well as a “convergence of evidence” approach, provide useable information despite
196 the above-mentioned uncertainties. A convergence of evidence approach that draws on (quasi-)
197 independent sources of information is useful to understand actual conditions. For convergence of
198 Earth observations, hydrologic models can generate ensembles of historical, current, or future
199 estimates of snow, streamflow, soil moisture, and evapotranspiration, which can then be compared
200 to satellite derived estimates of surface water (e.g., McNally et al., 2019), soil moisture (e.g.,
201 McNally et al., 2016), vegetation conditions and evapotranspiration (e.g., Jung et al., 2019; Pervez
202 et al., 2021), snow cover (e.g., Arsenault et al., 2014), in situ streamflow (e.g. Jung et al., 2017) and
203 others. Hydrologic estimates can also be compared to outcomes in crop production (e.g., (e.g.,
204 McNally et al., 2015; Davenport et al., 2019; Shukla et al., 2020), and nutrition, health, and food
205 security (e.g., Grace and Davenport, 2021) to provide a qualitative understanding of both hydrologic
206 model performance and conditions on the ground. In this paper we provide an example for 2018

207 where drought conditions were associated with crisis levels of acute food insecurity over most of
208 Afghanistan (FEWS NET, 2018c).

209
210 To summarize, our experience and the literature have characterized uncertainties in available
211 meteorological forcing for the region. GDAS, CHIRPS, and MERRA-2 were chosen for the FLDAS
212 system based on our project requirements of (a) a sufficiently long historical record for
213 contextualizing estimates in terms of anomalies (b) low latency (< 1-month) for timely decision
214 support, (c) familiar to the FEWS NET user-community, and (d) prior evaluation by our team and
215 the broader community. We note here and describe in more detail later that the Integrated Multi-
216 satellite Retrievals for the Global Precipitation Mission (IMERG), a NASA precipitation product
217 (Huffman et al., 2020) also meets these requirements, since version 6 which was released in 2019
218 (after these studies and initial FLDAS configuration). We will describe IMERG, GDAS, and
219 MERRA-2 comparison in the Results (Section 3).

220 **2 Methods**

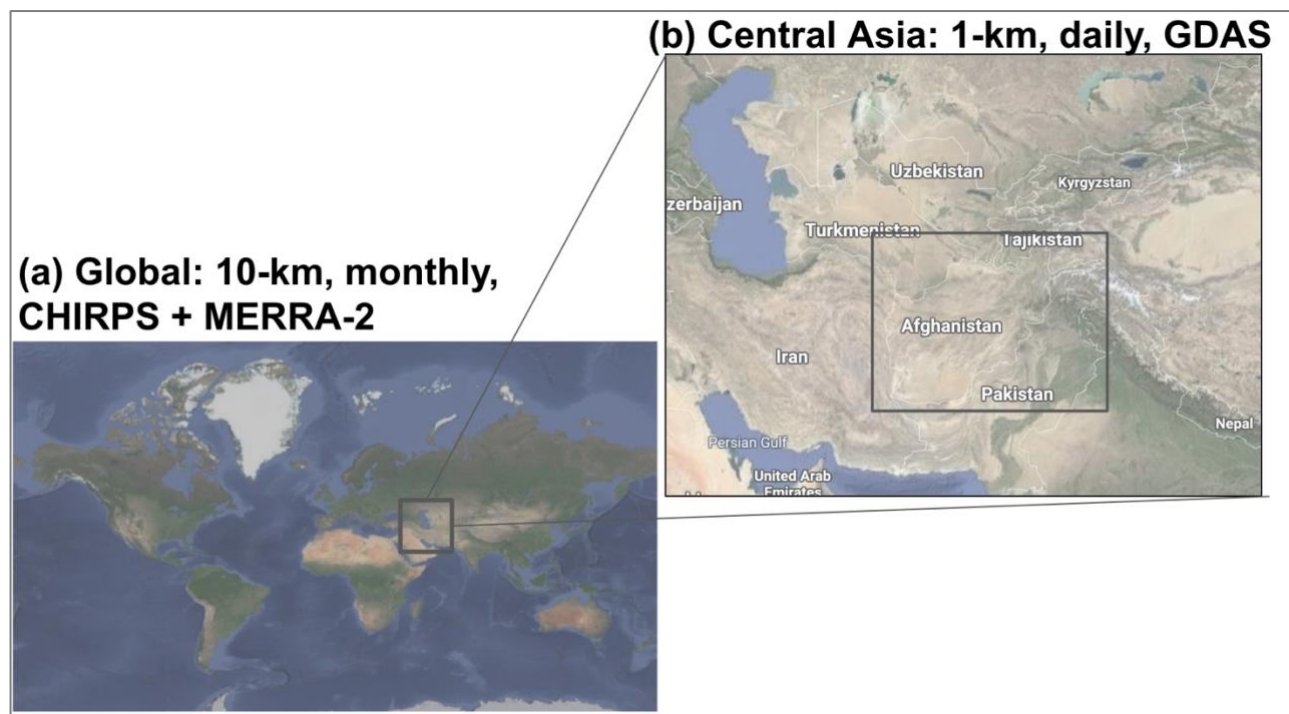
221 **2.1 Land Surface Modeling System & Parameters**

222 A land surface model (LSM) can provide spatially and temporally continuous information about the
223 water and energy budgets of the land surface. This information is useful for food and water security
224 applications in places where in situ measurements of rainfall, soil moisture, snow and runoff are
225 sparse. This is particularly relevant in mountainous places like Afghanistan where heterogeneous
226 geography limits the representativeness of sparse in situ measurements. The FLDAS (McNally et
227 al., 2017) utilizes the NASA's Land Information System Framework (LISF), which is composed of
228 a pre-processor, the Land surface Data Toolkit (Arsenault et al., 2018), the Land Information
229 System (Kumar et al., 2006; Peters-Lidard et al., 2007), and the Land Verification Toolkit (Kumar
230 et al., 2012). In this data descriptor we describe the two configurations of the FLDAS data streams
231 used for Central Asia food and water security applications. It uses the Noah 3.6 LSM (Chen et al.,
232 1996; Ek et al., 2003) for the two data streams (Fig. 3 and Table 1). The first data stream is global,
233 at ~1 month latency, and provides monthly average outputs on a 10-km grid from 1982-present. The
234 second data stream centered on Central Asia, ~1 day latency, provides daily average outputs at 1-km
235 from 2001-present.

236
237 One important feature, added by the NASA LISF software development team, is the radiation
238 correction described in Kumar et al. (2013), which improves the representation of snow dynamics
239 with respect to slope and aspect corrections on the downward solar radiation field. Another
240 noteworthy feature is the method of the Central Asia data stream restart (i.e., annual initialization
241 based on climatology), which was developed to address an issue of excessive inter-annual snow
242 accumulation found in the Noah LSM. First, a nine-year spin-up of the system was performed to
243 produce stable snow and soil moisture conditions. Next, the resulting model states were compared
244 with the Moderate Resolution Imaging Spectroradiometer (MODIS) Maximum Snow Extent data

245 originally computed by NOAA National Operational Hydrologic Remote Sensing Center (Greg Fall,
246 NOAA Operational Data Center, written communication., 2014) . Then, the model-estimated
247 conditions were adjusted to produce a climatological model state for 1 October that is used to
248 initialize each year. This approach ensures that the ‘water year,’ beginning 1 October, is initialized
249 with a reasonable initial amount of snowpack. While this method does effectively manage excessive
250 inter-annual modeled snow accumulation, the user should be aware that using the climatological
251 model state will persist for ~1-2 months in the water and energy balance of the LSM until they are
252 superseded by “observed” meteorological inputs for the current water year. Preliminary work
253 indicates that this issue will be resolved in future updates. In contrast, the global data stream does
254 not use this 1 October initialization procedure.

255 Although the two data stream specifications are largely the same, there are some differences related
256 to the input forcings, parameters and specifications (Table 1) and also model spin-up procedures.
257



258
259 Figure 3. The FEWS NET Land Data Assimilation System (FLDAS) domains for (a) the global data
260 stream at 10-km spatial resolution and ~1 month latency for monthly averaged hydrologic estimates
261 and (b) the Central Asia data stream at 1-km spatial resolution and ~1 day latency for daily averaged
262 hydrologic estimates.

263
264 Table 1. FEWS NET Land Data Assimilation System (FLDAS) specifications for (A) global data
265 stream, 10-km monthly with CHIRPS+MERRA-2; and (B) Central Asia data stream, 1-km, daily
266 with GDAS.

	Global	Central Asia
Spatial Extent	179.95°W- 179.95°E, 59.95°S-89.95°N	30-100°E, 21-56°N
Landmask	Generated from MODIS using LISF-LDT, with MOD44w mask applied post-processing.	MOD44w (Carroll et al., 2017)
Landcover	IGBP landcover	IGBP landcover
Elevation	Shuttle Radar Topography Mission SRTM (NASA JPL, 2013)	SRTM
Albedo	National Centers for Environmental Prediction (NCEP) albedo (Csiszar and Gutman, 1999) & MODIS-based Max Snow Albedo (Barlage et al., 2005)	NCEP albedo & MODIS-based Max Snow Albedo
Vegetation Parameters	NCEP greenness fraction (Gutman and Ignatov, 1998)	NCEP greenness fraction
Non-Precipitation Meteorological Inputs	MERRA-2	GDAS
Soil Texture	Food and Agricultural Organization (FAO) soil texture & properties (Reynolds et al., 2000)	FAO soil texture & properties
Precipitation Inputs	CHIRPS daily precipitation, downscaled to 6-hourly with LDT	GDAS 3-hourly precipitation
Specifications	Noah 3.6.1	Noah 3.6.1
Map Projection	Geographic Latitude-Longitude	Geographic Latitude-Longitude
Software Version	7.2	7.3
Spatial Resolution	10-km	1-km
Temporal Coverage	1982-01-01 to present	2000-10-01 to present
Model Timestep	15-min timestep	30-min timestep
Met. Forcing Heights	2-m Air Temperature (Tair), 10-m Wind	2-m Tair, 10-m Wind
Soil layers (meters)	0-0.1; 0.1-0.4; 0.4-1.0; 1-2	0-0.1; 0.1-0.4; 0.4-1.0; 1-2

Features	radiation correction	radiation correction
----------	----------------------	----------------------

267

268 The parameters and specifications listed in Table 1 are largely default settings defined by the Noah
 269 LSM community (NCAR Research Applications Library, 2021). Ongoing research aims to identify
 270 where model output performance can be improved with parameter updates. Evaluating parameter
 271 updates had similar challenges as evaluating input forcing described in Section 1.2: without reliable
 272 reference data it is difficult to determine a “best” input. For example, we have explored changing
 273 soil parameters from FAO to International Soil Reference and Information Centre (ISRIC) SoilGrids
 274 database (Hengl et al., 2017). This change did not result in improvements in streamflow statistics in
 275 southern Africa, nor in soil moisture anomalies’ ability to represent drought events. We expect
 276 similar results in Afghanistan where, e.g., streamflow will be sensitive to a change in soil
 277 parameters and the lack of referenced data to evaluate if there is an improvement. Moreover, our
 278 model runs at 0.1 and 0.01 degrees may not fully exploit the added value of the 250m soil grids as
 279 noted in Ellenburg et al. (2021) for a LISF application in East Africa.

280 Vegetation parameters are also potential sources of improvement whose importance to LDAS
 281 hydrologic estimates has been highlighted (e.g., Miller et al., 2006). We have found the NCEP
 282 estimates of green vegetation fraction (GVF) to be sufficient for this configuration of Noah 3.6. We
 283 found that a time series of GVF derived from the Normalized Difference Vegetation Index (NDVI)
 284 did not improve representation of droughts in eastern Africa. However, future FLDAS global and
 285 Central Asia versions can be run with Noah-Multi parameterization (Noah-MP) (Niu et al., 2011)
 286 which has multiple vegetation options and relies on either Leaf Area Index rather or GVF. This
 287 model update is expected to open possibilities for choice of datasets to meet our application needs
 288 and potentially improve representation of the water balance.

289 **2.2 Meteorological Forcing Inputs**

290 As previously discussed, precipitation is a critical input to land surface models. The lower-latency
 291 Central Asia data stream is a daily product, forced with GDAS (Derber et al., 1991) 3-hourly
 292 precipitation, which is available from 2001 to present at <1-day latency. This dataset was chosen
 293 because of its latency. The global data stream is driven by the daily CHIRPS product (Funk et al.,
 294 2015), which is available from 1981 to present at ~ 5-day latency for CHIRPS Preliminary and ~1.5-
 295 month latency for CHIRPS Final. The CHIRPS products were chosen as inputs because of their
 296 proven performance in the literature, which has made it the “gold standard” for food and water
 297 security monitoring by organizations like FEWS NET, the World Food Program, and others who
 298 need up-to-date estimates and a 40+ year historical record. As mentioned earlier, lack of rainfall
 299 stations for bias correction of satellite-derived estimates and evaluation poses a major challenge.
 300 However, we find that the GDAS rainfall product and the CHIRPS rainfall product are adequate for
 301 routine monitoring and, along with additional sources of remote sensed information, are important
 302 for convergence of evidence when making a best estimate at land surface states and fluxes.
 303

304 Before the daily CHIRPS rainfall data can be used as input to the FLDAS models, the daily
305 precipitation is pre-processed to a sub-daily timestep, using the LDT component of the LISF
306 software. LDT temporally disaggregates the daily CHIRPS rainfall using an approach similar to the
307 North American LDAS precipitation temporal downscaling (Cosgrove et al., 2003). For this
308 approach, we use a finer timescale MERRA-2 precipitation timescale as a reference dataset to
309 represent an accurate diurnal cycle. We note that this step in our methodology facilitates the solving
310 of FLDAS water and energy balances at a sub-daily timestep. However, for Central Asia we do not
311 have sufficient reference data available to assess the importance of sub-daily precipitation
312 distribution, as was demonstrated by Sarmiento et al. (2021) for the United States where adequate
313 reference data are available. For spatial downscaling, coarser scale meteorological forcings are
314 spatially disaggregated to the output resolution (0.01, and 0.1 degree for Central Asia and global,
315 respectively) in the LISF using bilinear interpolation.

316 The FLDAS models require additional meteorological inputs, including air temperature, humidity,
317 radiation, and wind. The lower-latency Central Asia data stream uses GDAS 3-hourly
318 meteorological inputs available from 2001-present at <1-day latency. For a longer historical record,
319 the global data stream uses MERRA-2 (Gelaro et al., 2017) (1979-present) 1-hourly products with a
320 two-week latency. Over the Afghanistan domain GDAS temperature has an upward trend, whereas
321 MERRA-2 is consistently warmer before 2010. We find that GDAS and MERRA-2 temperature
322 estimates are of similar magnitude during 2011-2020. Similar results were noted by Yoon et al.
323 (2019) who found an upward trend in GDAS temperature, as well as consistently higher
324 temperatures in MERRA-2 across a broad High Asia domain.

325 **2.3 Model Evaluation Statistics and Comparison Data**

326 In addition to guidance from previous studies (Section 1.2), we assessed the quality of our modeling
327 outputs by conducting comparisons between (1) FLDAS satellite rainfall inputs and other satellite
328 precipitation estimates, and (2) model estimated snow cover fraction and satellite derived snow
329 cover fraction estimates.

330
331 For the precipitation analysis, we compare CHIRPS and GDAS inputs to the Integrated Multi-
332 satellite Retrievals for the Global Precipitation Mission (IMERG), a NASA precipitation product
333 that integrates passive microwave and infrared satellite data with surface station observations
334 (Huffman et al., 2020). The IMERG Final Run precipitation product, available at ~ 2-month latency
335 (thus not suitable for our monitoring applications) has been used in numerous verification studies,
336 including studies over Africa (Dezfuli et al., 2017), South America (Gadelha et al., 2019; Manz et
337 al., 2017), and the mid-Atlantic region of the United States (Tan et al., 2016). These studies
338 demonstrated that IMERG Final Run was able to capture large spatial patterns and seasonal and
339 interannual patterns of rainfall. However, fewer studies have explored the performance of the lower
340 latency IMERG Late Run (doi: 10.5067/GPM/IMERGDL/DAY/06) product that we use here.
341 Kirshbaum et al. (2016) include a qualitative comparison for CHIRPS Final and IMERG Late Run
342 for the Southern Africa start-of-season 2015. IMERG Late Run appears to perform similarly to the

343 1.5-month latency CHIRPS Final and outperform the 1-day latency NOAA Rainfall Estimate
344 version 2 (RFE2) product (Xie and Arkin, 1996). Differences in the daily rainfall distribution
345 patterns between IMERG Final Run and CHIRPS Final have also been shown to affect the resulting
346 hydrological modeled output in simulations done using the NASA LISF (Sarmiento et al., 2021).

347
348 For the snow cover fraction (SCF) analysis, we compare the global and Central Asia data streams
349 with the MODIS daily SCF product, MOD10A1 Collection 6 (Hall and Riggs, 2016). MOD10A1
350 data are available at 500-m spatial resolution from February 2000 to the present. SCF is generated
351 using the Normalized Difference Snow Index (NDSI) and additional filters to reduce error and flag
352 uncertainty. Routine qualitative comparisons, which can be viewed on the NASA LISF FEWS NET
353 project website, generally show agreement between the model and MODIS SCF, as well as
354 occurrence of cloud cover (<https://ldas.gsfc.nasa.gov/fldas/models/central-asia>). Following
355 Arsenault et al. (2014), we aggregated pixels to 0.01 degree to reduce error related to sensor viewing
356 angles and gridding artifacts. For this analysis, using MODIS SCF as “truth,” we determined True
357 Positives (TP), True Negatives (TN), False Negatives (FN) and False Positives (FP). We then
358 computed probability of detection (POD) where $POD = (TP / (TP + FN))$ and False Alarm Rate
359 (FAR) where $FAR = (FP / (FP + TN))$. We computed these for the total area of Afghanistan (60-76E,
360 28-39N), as well as by basin (Fig. 4). This paper does not compare modeled snow water equivalent
361 (SWE) to independent snow observations because, as noted by Yoon et al. (2019), direct evaluation
362 of snow mass and SWE) is difficult over Central Asia due to poor coverage of accurate snow
363 observations. We follow the Yoon et al. (2019) recommendation to conduct quantitative SCF
364 comparisons and provide qualitative SWE analysis in Applications, Section 4.

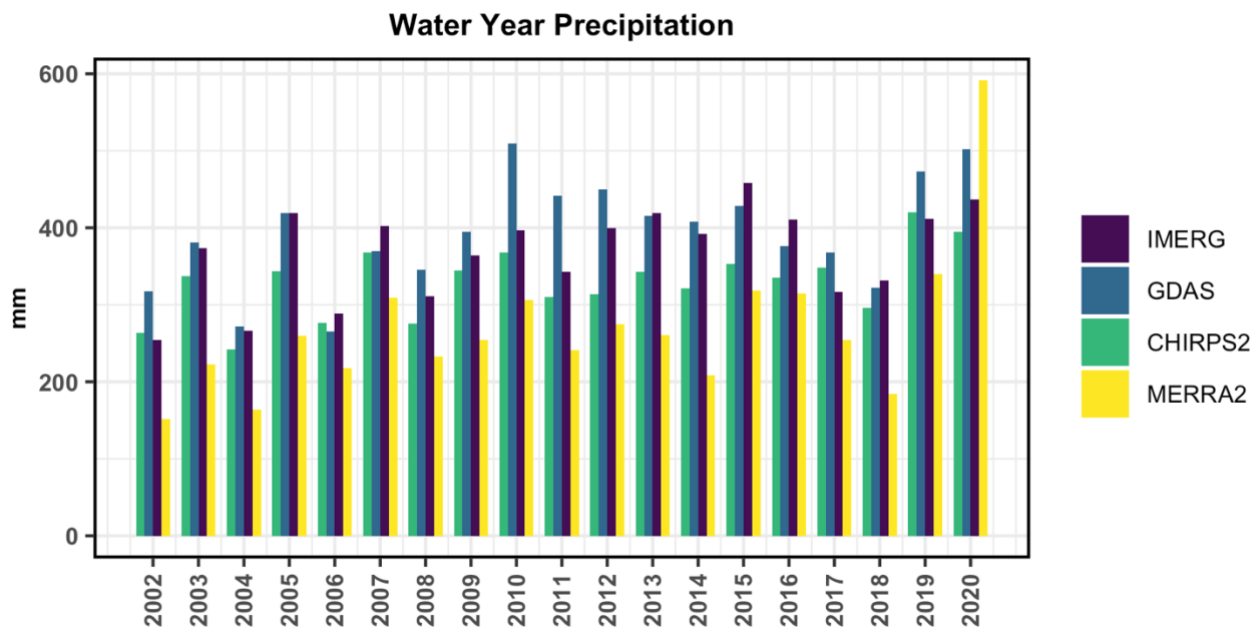
365
366 In addition to rainfall and snow comparisons, we conducted monthly pixel-wise comparison of
367 Central Asia and the global run’s estimates of evapotranspiration (ET) and soil moisture versus
368 Operational Simplified Surface Energy Balance (SSEBop, (Senay et al., 2013)). ET and Soil
369 Moisture Active Passive (SMAP) Level 3 (Entekhabi et al., 2010, 2016) using the Normalized
370 Information Contribution (NIC) metric following Sarmiento et al., (2021). The analysis was
371 performed for the period 2016-2021 to match the SMAP record. The NIC metric first computes
372 anomaly correlations between the model runs and the reference dataset and then computes the
373 difference between the performance of each model run using a scale of -1 to +1 to highlight if the
374 global or Central Asia data stream performs better with respect to the reference. To make the
375 comparisons, the reference datasets (SMAP and SSEBop) were re-gridded to match the grid spacing
376 and locations of the experiment model outputs.

377 **3 Results**

378 **3.1 Gridded Rainfall Comparison**

379 We have two data streams for Central Asia applications with different precipitation inputs: 1) the
380 global data stream with CHIRPS precipitation at 10-km spatial resolution provides a long-term
381 consistent data record; and 2) the Central Asia data stream with GDAS precipitation at 1-km

382 provides near real time, finer spatial resolution updates. These two data streams have their
 383 respective errors and allow data users to apply a convergence of evidence approach for food and
 384 water security applications. This section presents a comparison of the GDAS, and CHIRPS
 385 precipitation inputs used for the Central Asia and global data streams, respectively. We also include
 386 IMERG Late Run for comparison as a high quality, low latency product. Future work may
 387 incorporate the IMERG Late Run precipitation inputs into FLDAS simulations. We also include
 388 MERRA-2 precipitation for comparison. Pair-wise correlations are shown in Table 2. CHIRPS
 389 Final, IMERG Late Run and GDAS ($R \geq 0.90$) are well correlated in terms of average daily
 390 precipitation (mm/day) at the monthly and annual (i.e., water year) timestep. MERRA-2 correlations
 391 with these datasets are lower at the monthly ($0.75 \leq R \leq 0.81$) and water year ($0.64 \leq R \leq 0.69$)
 392 timesteps. Fig. 4 shows the time series of the precipitation products for their overlapping period of
 393 record (2001-2020), which illustrates how they vary in time, and shows some general patterns in
 394 terms of relative precipitation in mm: GDAS (blue) and IMERG Late Run (purple) tend to have the
 395 highest precipitation totals, CHIRPS (green) has lower precipitation but is higher than MERRA-2
 396 (yellow) which tends to have the lowest precipitation, until 2019 when it is notably higher than the
 397 other products.
 398



399
 400
 401 Figure 4. Afghanistan water year precipitation for CHIRPS, GDAS, IMERG Late Run, and
 402 MERRA-2.

403
 404 Table 2. Afghanistan spatial average Spearman Rank Correlation (R) of monthly (water year)
 405 precipitation 2001-2020

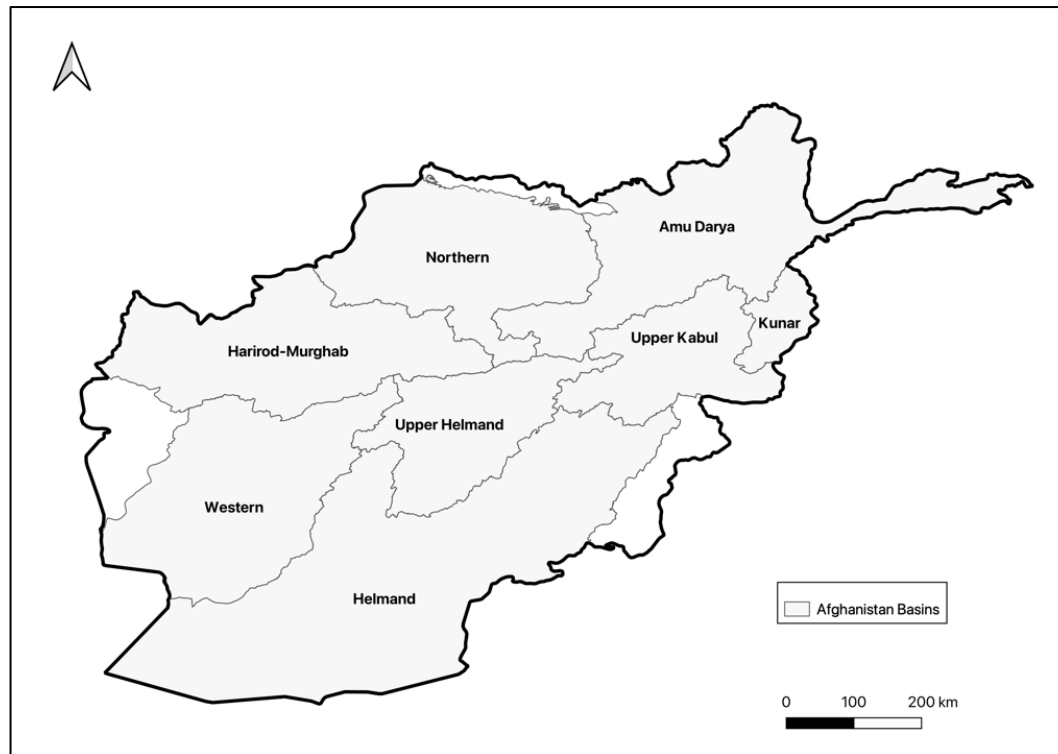
	GDAS	CHIRPS Final	IMERG Late Run
--	------	--------------	----------------

GDAS	x	-	-
CHIRPS Final	0.91 (0.92)	x	-
IMERG Late Run	0.91 (0.89)	0.92 (0.90)	x
MERRA-2	0.75 (0.64)	0.78 (0.68)	0.81(0.69)

406

407 3.2 Remotely Sensed and Modeled Snow comparisons

408 The estimation of snow is important for Afghanistan and Central Asia because it is a critical
 409 contributor to water resources and irrigated agriculture. We compared average SCF (Fig. 6a), POD,
 410 and FAR statistics (Fig. 6b) relative to MODIS SCF over eight hydrologic basins in Afghanistan.
 411

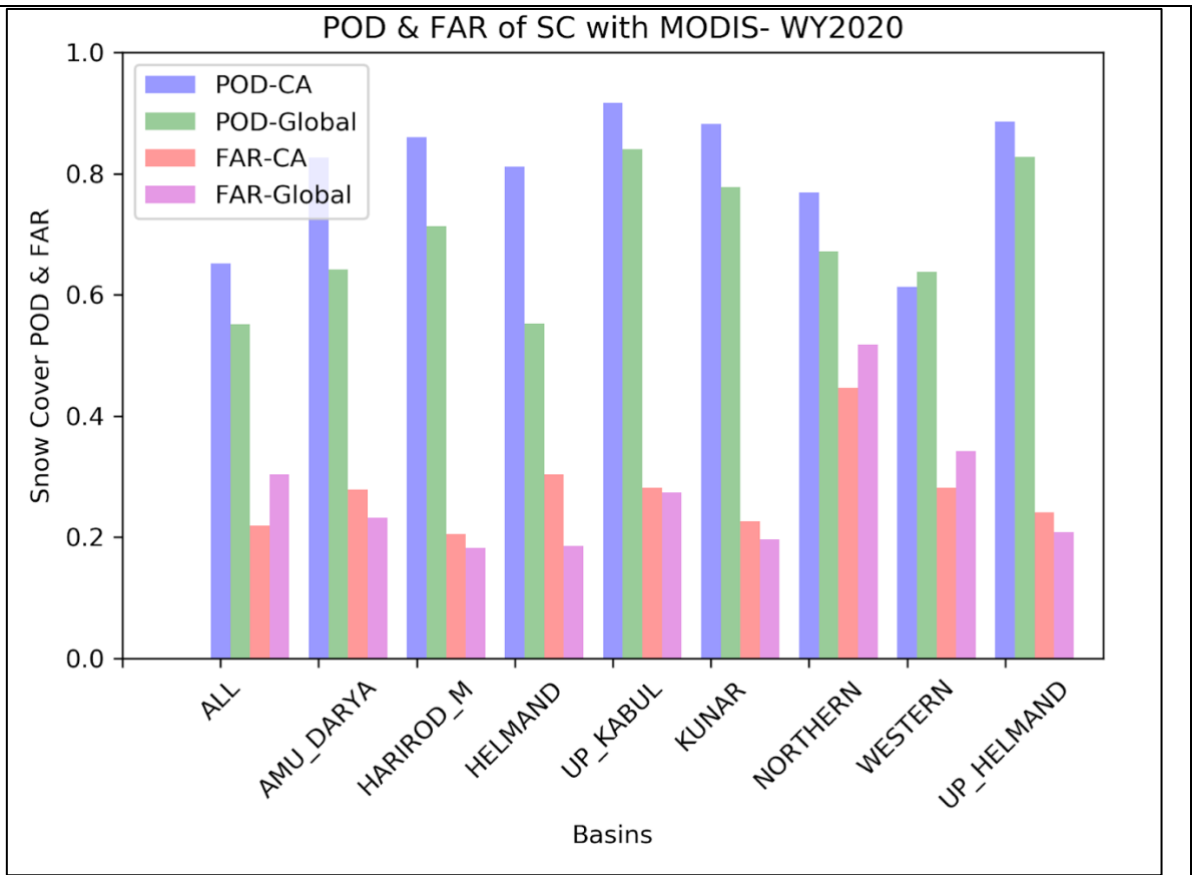


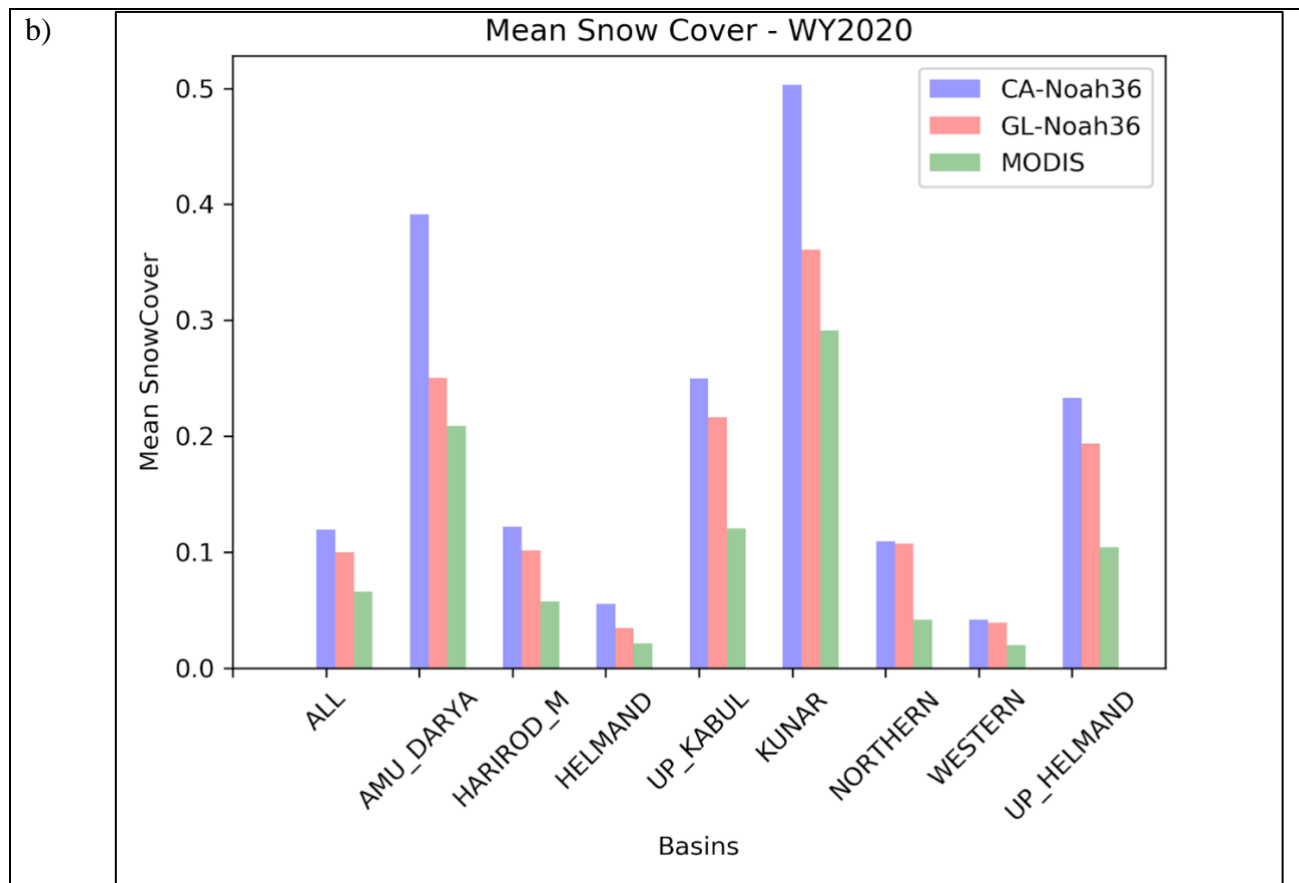
412

413 Figure 5. Hydrologic basins used in the analysis of categorical statistics for snow covered fraction.
 414

414

a)





415 Figure 6. (a) Mean snow cover fraction for the entire area and by hydrologic basin for MODIS
 416 Snow Cover Fraction (SCF), Central Asia (CA) and global (GL) data streams for water year 2020.
 417 (b) Probability of Detection (POD) of snow presence, and False Alarm Rate (FAR) for the Central
 418 Asia (CA) and global data streams relative to the MODIS SCF for water year 2020.

419
 420 Overall, both model runs estimate greater average SCF than the MODIS SCF product. The Central
 421 Asia data stream has consistently higher average snow cover for all basins compared to MODIS
 422 SCF estimates and the global data stream. Perhaps not surprisingly that the Central Asia data stream
 423 performs consistently better in POD (by basin = ~80%) except for the Western Basin. Similarly, the
 424 FAR of the Central Asia data stream is higher where POD is higher except for the Northern Basin.
 425 The difference in statistics may be related to the different forcing inputs or the higher spatial
 426 resolution of the Central Asia data stream. Kumar et al. (2013) note that higher spatial resolution
 427 was important for snow dominated basins.

428
 429 In addition to precipitation and snow cover comparisons we conducted comparisons with remotely
 430 sensed soil moisture and ET (not shown). We found that in general, GDAS derived estimates of ET
 431 consistently performed better over Afghanistan in terms of pixel-wise anomaly correlation and NIC
 432 with SSEBop ET. Meanwhile, neither modeled estimate of soil moisture consistently outperformed

433 the other with respect to SMAP. The ET results lend some support to the quality of the Central Asia
434 data stream estimates. However, the lack of signal in the soil moisture comparisons suggests that
435 more careful analysis of the model and remote sensing errors is required before drawing conclusions
436 regarding which data stream is “best.”

437 **3.3 Discussion of results compared to previous studies**

438 Despite the lack of ground-based observations, our analysis shows that the remotely sensed
439 estimates and the models have good correspondence with other sources of evidence in terms of
440 seasonal timing and performance. This provides analysts with confidence when using the FLDAS
441 snow estimates, in tandem with other sources, as an input to food security assessments. Our
442 approach is supported by other studies that have explored the challenges of evaluating hydrologic
443 estimates over the region (Immerzeel et al., 2015; Ghatak et al., 2018; Yoon et al., 2019; Qamer et
444 al., 2019).

445
446 Yoon et al. (2019) show that their LSM ensembles of SCF have an average POD of 72% and FAR
447 of 36%, which is within the range of our POD and FAR statistics (60-80% POD; 20-40% FAR)
448 compared to MODIS SCF. The categorical statistics indicate that Central Asia (GDAS) tends to
449 have both a higher probability of detection and false alarm rate, indicating higher averages than
450 MODIS SCF and global (CHIRPS).

451
452 With respect to the soil moisture and ET comparisons, we found that the Central Asia data stream
453 estimates of ET were better correlated with SSEBop ET, but neither data stream was consistently
454 better correlated with SMAP. These differences could be a function of non-precipitation differences,
455 or higher spatial resolution. Ghatak et al. (2018) also found that the choice of reference dataset (with
456 its own characteristics and errors) was an important factor.

457
458 In general, given the lack of clarity on “best” FLDAS data stream, the convergence of evidence
459 approach allows us to consult both data streams, leveraging the longer time series of CHIRPS and
460 the lower latency of GDAS.

461 **3.4 Limitations and Future Developments**

462 Given the need for multiple data streams for convergence of evidence, we have summarized the pros
463 and cons of the Central Asia and global data streams in Table 3.

464

465 Table 3. Pros and cons of the two data streams

	Central Asia: Noah 3.6 with GDAS (2000-present)	Global: Noah 3.6 with CHIRPS+MERRA-2 (1982-present)
Pros	1-km	less computationally intensive

	1-day latency, daily timestep	longer time record
	Snow estimates available in USGS Early Warning eXplorer https://earlywarning.usgs.gov/fews/ewx/	CHIRPS & MERRA-2 forcing spatial resolution does not change over time (stable climatology)
		Water and Energy balance available in NASA GIOVANNI https://giovanni.gsfc.nasa.gov/giovanni/ ; Google Earth Engine https://developers.google.com/earth-engine/datasets/tags/fldas ; Climate Engine https://climateengine.com/
Cons	more computationally intensive	lower resolution (10-km)
	shorter time record	~30-day latency
	GDAS forcing resolution changes over time (unstable climatology) (NOAA NCEP https://www.emc.ncep.noaa.gov/gmb/STATS/html/model_changes.html)	not publicly available at daily timestep
	large data volume, difficult to move	

466

467 IMERG version 6 was released in 2019 and includes rainfall estimates processed back to 2000. Prior
468 to this change we had found encouraging results when comparing the onset of rainy season using
469 both IMERG Late Run and CHIRPS (Kirschbaum et al., 2016). However, at that time the period of
470 record was a limitation for computing anomalies. We now have an adequate period of record, and
471 IMERG Late Run is planned to be part of the upcoming FLDAS global and FLDAS Central Asia
472 releases. We are also encouraged by the quality of IMERG at the daily timestep when compared to
473 CHIRPS over the United States where accurate reference data are available (Sarmiento et al., 2021).
474

475 In addition to IMERG other promising rainfall datasets are in development. Ma et al. (2020) have
476 developed the AIMERG dataset that combines IMERG Final Run with the APHRODITE rain-gauge
477 derived product (Yatagai et al., 2012). Another promising dataset is CHIMES (Funk et al., 2022), a
478 blend of CHIRPS and IMERG, whose developers have been exploring the strengths and limitations
479 of these two datasets and their fusion to produce an optimal product.
480

481 With respect to other FLDAS developments, FLDAS global and Central Asia are planned to be
 482 transition to Noah-MP. This will allow for improved representation of snowpack and groundwater.
 483 This will also necessitate the use of different parameters, e.g., leaf area index, as well as the
 484 potential to explore different parameter sets like ISRIC soils. In the meantime, multi-forcing and
 485 multi-model ensembles, and convergence of evidence with other remotely sensed data and field
 486 reports, are a viable approach for providing hydrologic estimates for various applications.

487 **4 Applications**

488 These data from global and Central Asia data streams are routinely used in several FEWS NET
 489 information products listed in Table 4. NOAA’s Climate Prediction Center (CPC) International
 490 Desks provide a weekly briefing on the past week’s weather conditions and 1– 2-week forecasts for
 491 FEWS NET regions of interest, including Central Asia. There is also a monthly FEWS NET
 492 Seasonal Monitor and a monthly Seasonal Forecast Review for which these data provide
 493 information on the current state of the snowpack, soil moisture, and runoff. These “observed
 494 conditions” can then be qualitatively combined with forecasts 1 week to many months in the future
 495 to assess potential hydro-meteorological hazards. To demonstrate the role of these data in the early
 496 warning process, at different points in the season, we provide an example of the 2017-2018 wet
 497 season in Afghanistan during a La Niña event that contributed to drought.

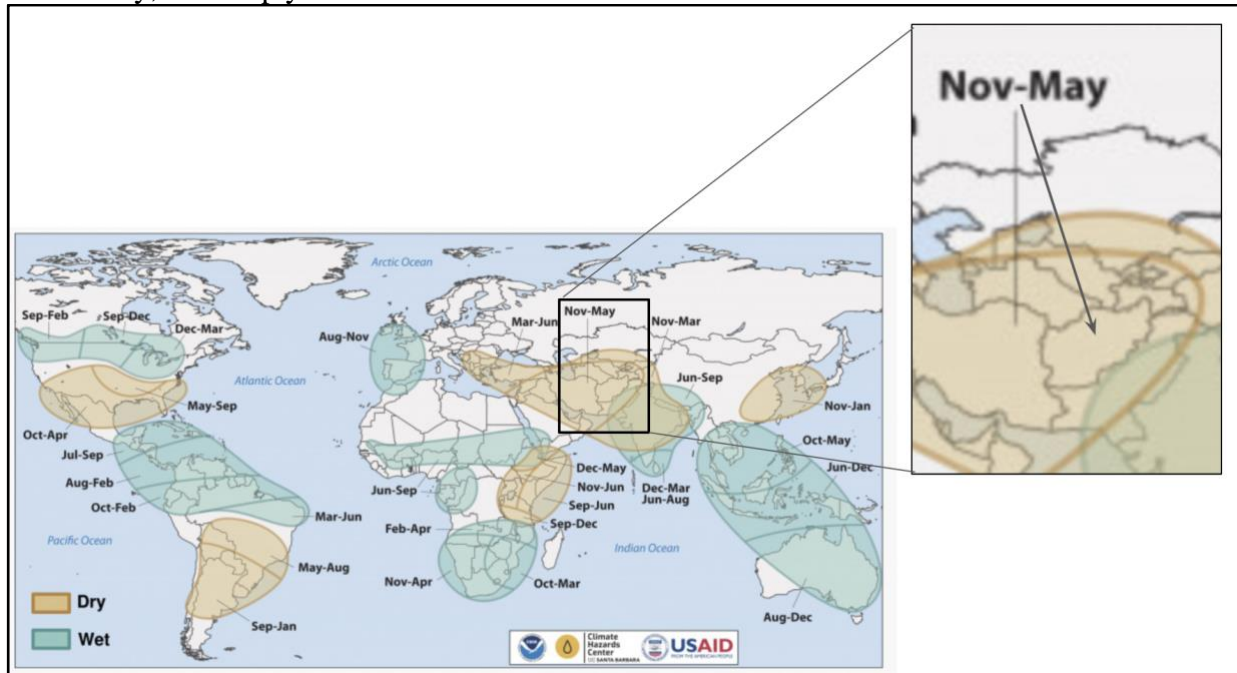
498
 499 Table 4. Routine Applications of FLDAS Central Asia’s Afghanistan hydrologic data.

Routine application of these data	Weblink to updates	Notes
FEWS NET Global Weather Hazards Summary produced by NOAA CPC	https://fews.net/global/global-weather-hazards/ https://www.cpc.ncep.noaa.gov/products/international/index.shtml	shapefiles https://ftp.cpc.ncep.noaa.gov/fews/weather_hazards/
Seasonal Monitor	https://earlywarning.usgs.gov/fews/afghanistan/seasonal-monitor	Updated near the middle of each month from October - May, the wet season.
FEWS NET Food Security Outlook Brief	https://fews.net/central-asia/afghanistan	Information on snow or other hydrology included if applicable
Crop Monitor for Early Warning	https://cropmonitor.org/index.php/cmreports/early-warning-report/	Information on early warning and crop conditions

500

501 **4.1 Snow Monitoring & Seasonal Outlooks**

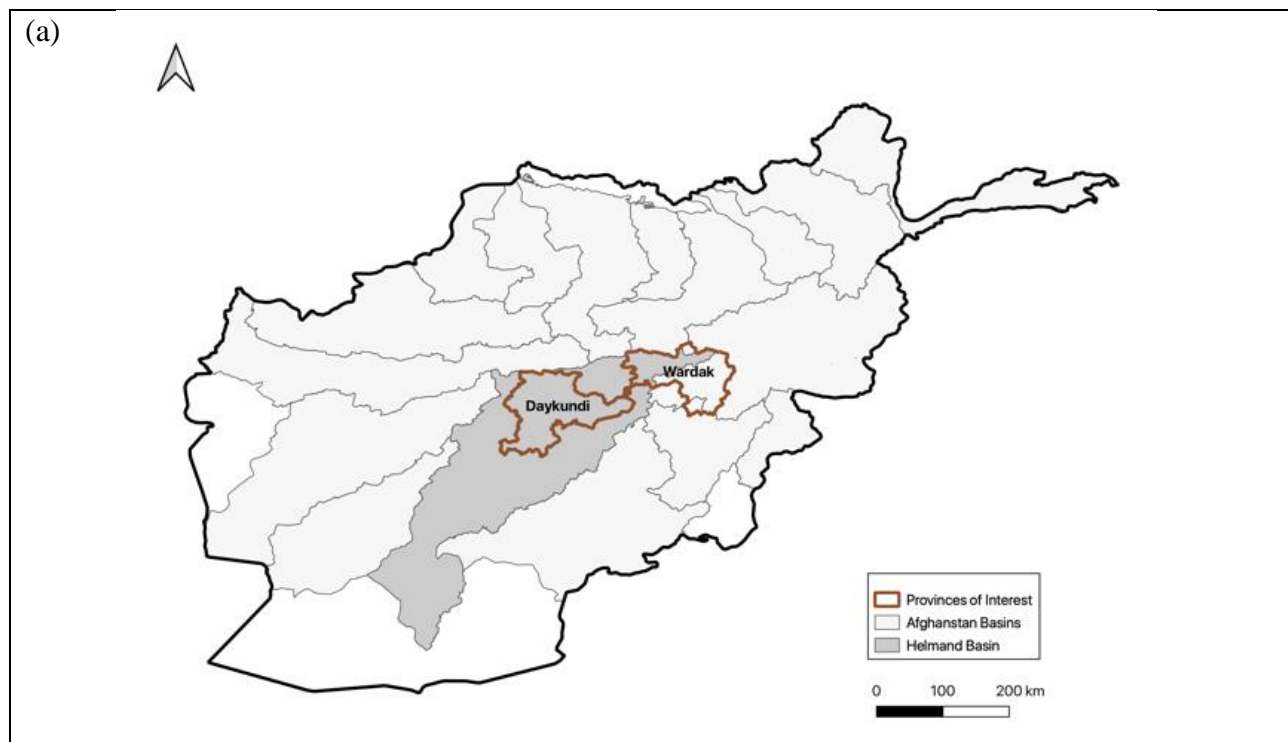
502 As previously mentioned, and as shown in Fig. 7, Afghanistan and the broader region is strongly
503 influenced by La Niña, which tends to increase the likelihood of below average precipitation.
504 Depending on this and antecedent conditions there is an increased likelihood of below average
505 snowpack, reduce springtime streamflow and flood risk, reduce summer irrigation water
506 availability, and crop yield losses.

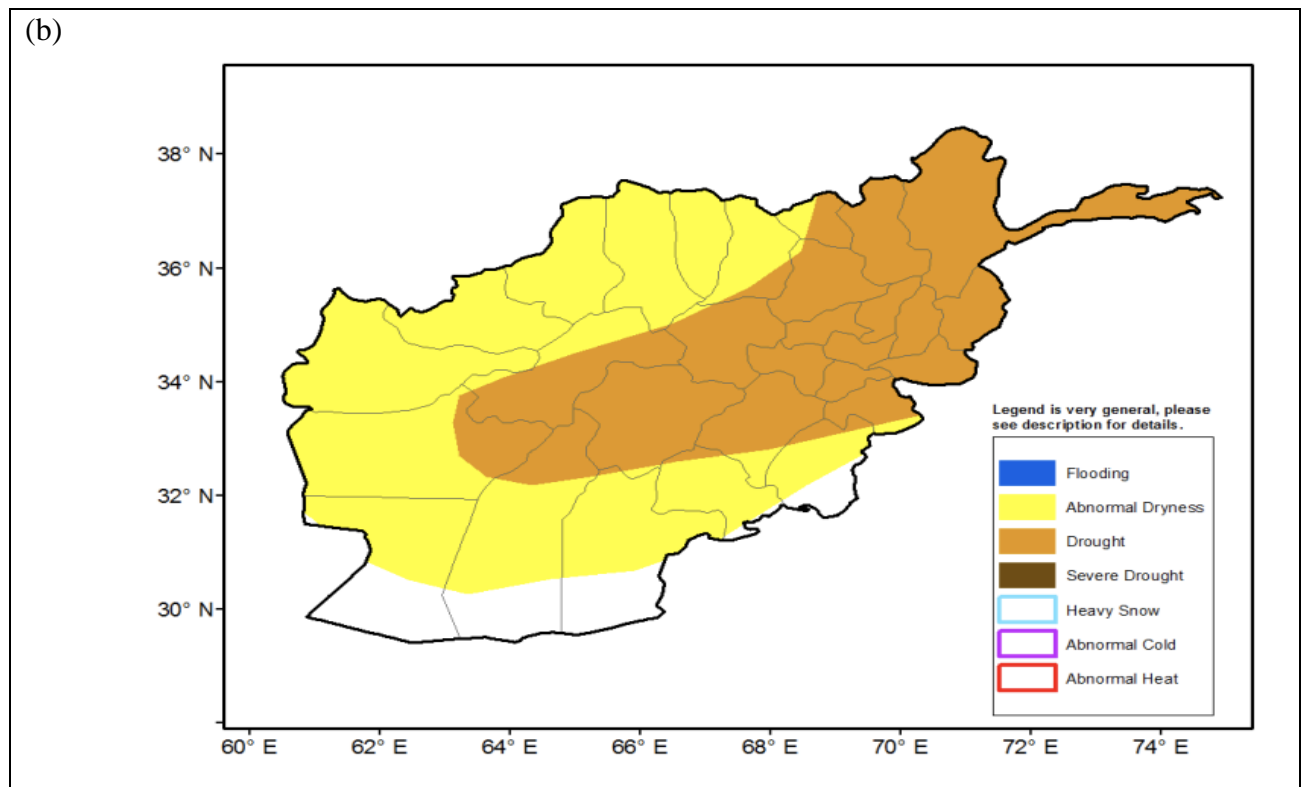


507
508 Figure 7. Timing of wet and dry conditions related to La Niña. Increased likelihood of dry
509 conditions from November-May for Afghanistan during La Niña events.

510
511 A La Niña Watch was issued by NOAA in September 2017 (NOAA, 2017). The FEWS NET
512 October 2017 Food Security Outlook (FEWS NET, 2017a) stated that La Niña conditions were
513 expected throughout the northern hemisphere fall and winter and that below-average precipitation
514 was likely over much of Central Asia, including Afghanistan, during the 2017-2018 wet season.
515 With the expectation of below average precipitation coupled with above average temperatures,
516 FEWS NET anticipated that snowpack would most likely be below average. In the context of food
517 security outcomes, it was assumed that areas planted with winter wheat were likely to be less than
518 usual, reducing land preparation activities and associated demand for labor. Two provinces of
519 particular concern were Daykundi and Wardak (Fig. 8a brown borders), both located in the
520 Helmand River Basin (Fig. 8a; gray shading). Precipitation deficits in these provinces would lead to
521 poor rangeland resources and pasture availability and would likely result in decreased livestock
522 productivity and milk production through May. However, given that October was the start of the wet
523 season, there remained a large spread of possible outcomes: spatial and temporal rainfall
524 distributions, and snowpack totals necessitating routine updates to assumptions.

525
526 Monitoring continued during the wet season, tracking observations from remote sensing, models,
527 and field reports as well as forecasts across timescales. This information was used to regularly
528 update expectations of end of season outcomes. Using the FLDAS Central Asia data stream, a
529 December 21, 2017, NOAA CPC Weather Hazards Brief reported that parts of northern and central
530 Afghanistan remained atypically snow free, and north-eastern high elevation areas exhibited SWE
531 deficits. SWE is a commonly used measurement of the amount of liquid water contained within the
532 snowpack, and an indicator of the amount of water that will be released from the snowpack when it
533 melts. By January 17, 2018, an abnormal dryness polygon was placed over northeastern Afghanistan
534 and the central highlands, based on below-average SWE values from the FLDAS Central Asia
535 estimates. Abnormal dryness is defined for an area that has registered cumulative 4-week
536 precipitation and soil moisture ranking less than the 30th percentile, with a Standardized
537 Precipitation Index (SPI) of 0.4 standard deviation below the average. In addition, it is required that
538 forecasts indicate below-average precipitation (less than 80% of normal) for that area during the 1-
539 week outlook period. By late February 2018, precipitation deficits and related SWE (Fig. 9)
540 increased and met the criteria for “drought” (Fig. 8b). Drought is defined as an area that has
541 previously been defined as “Abnormal Dryness” and has continued to register seasonal precipitation
542 and soil moisture deficits since the beginning of the rainfall season. Specifically, an eight-week
543 cumulative precipitation, soil moisture, and runoff below the 20th percentile rank, and an SPI of 0.8
544 standard deviation below the average are classification guidelines.
545

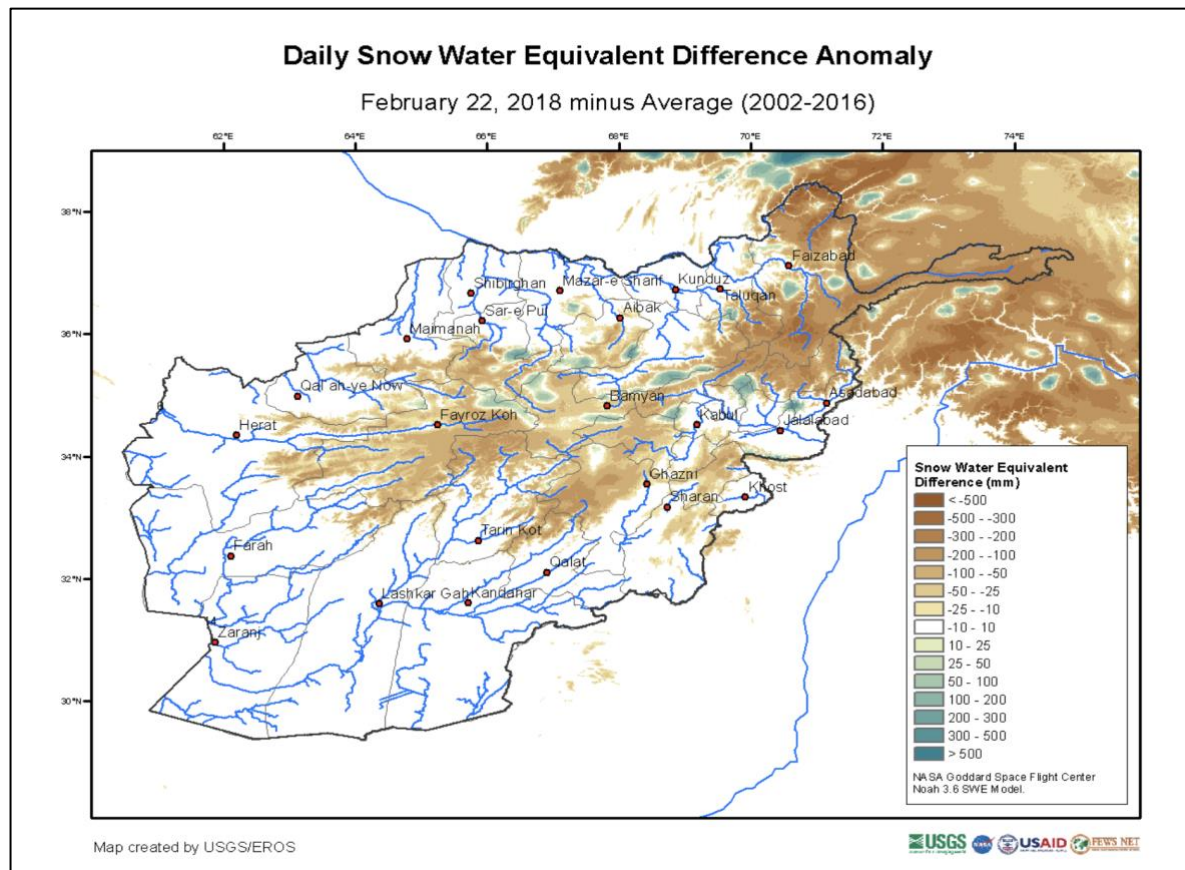




546

547 Figure 8. (a) Map showing hydrological basins, with Helmand Basin in darker gray and location of
 548 Daykundi and Wardak provinces (outlined in red) where food security conditions were of particular
 549 concern, (b) NOAA CPC Afghanistan Hazards Report for February 22-28, 2018 (CPC NOAA,
 550 2018) showing widespread abnormal dryness and drought, defined by 90-day precipitation deficits
 551 and extremely low snow water equivalent.

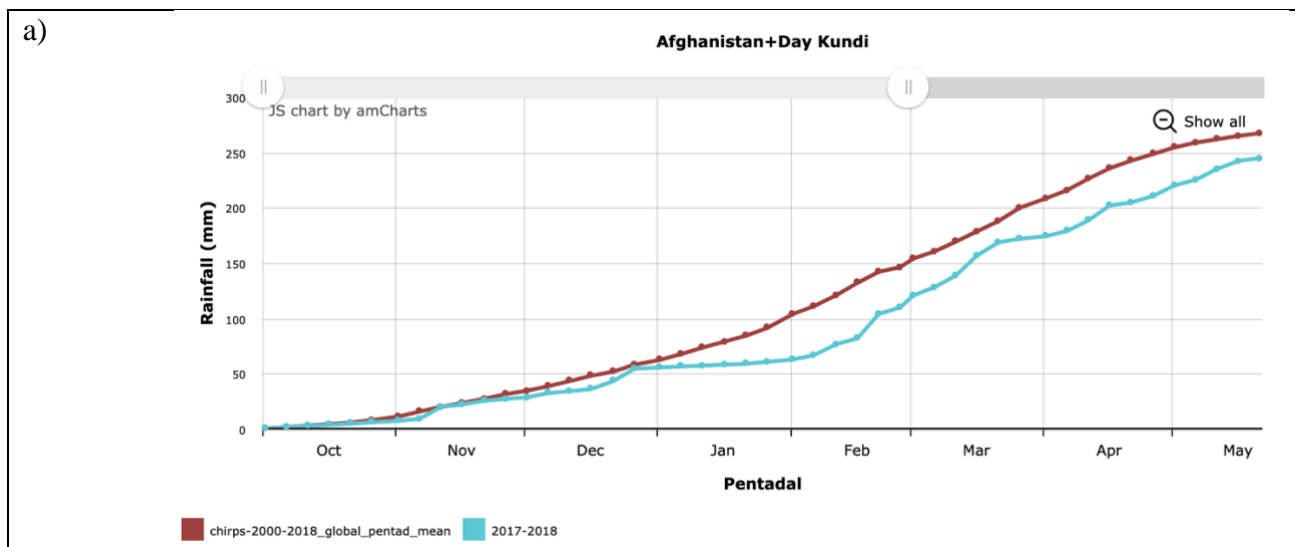
552



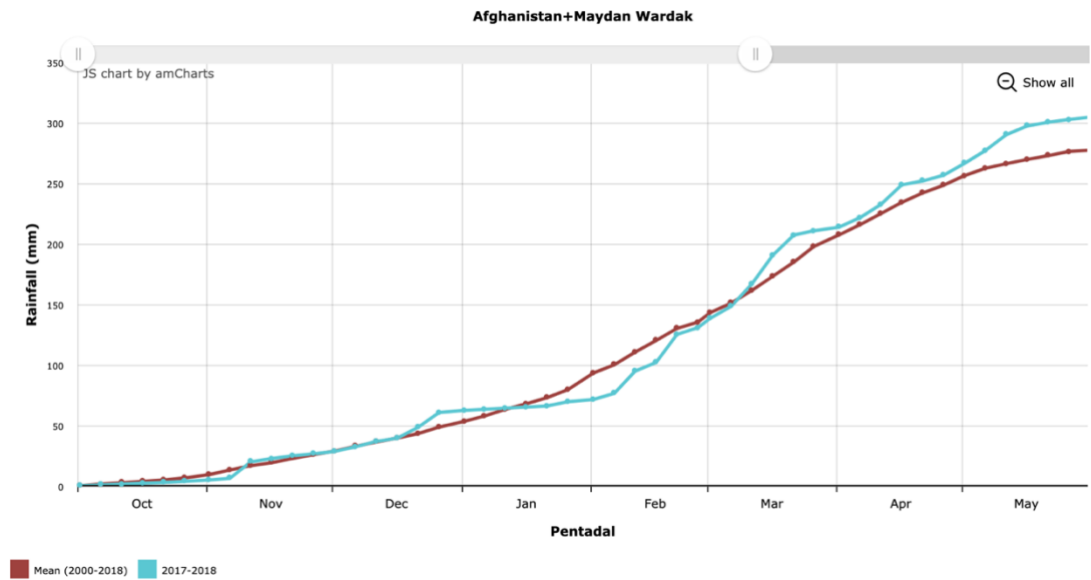
553
 554 Figure 9. FLDAS Central Asia snow water equivalent (SWE) estimates for February 22, 2018.
 555 SWE deficits of 300-mm were widespread at this time.

556
 557 The February 2018 Food Security Outlook (FEWS NET, 2018b) provided the following updates,
 558 based on the CPC Hazards Reports and Seasonal Monitors: “Snow accumulation and cumulative
 559 precipitation were well below average for the season through February 2018, with some basins at or
 560 near record low snowpack, with data since 2002....These factors will likely have an adverse impact
 561 on staple production in marginal irrigated areas and in many rainfed areas. [Moreover, with]
 562 forecasts for above-average temperatures during the spring and summer, rangeland conditions are
 563 expected to be poor during the period of analysis through September 2018. This could have an
 564 adverse impact on pastoralists and agro-pastoralists, particularly in areas where livestock
 565 movements are limited by conflict.” The Crop Monitor for Early Warning reports for February and
 566 March 2018 (GEOGLAM, 2018a, b) also cited reduced snowpack in Afghanistan and the negative
 567 impacts on winter wheat crops as well as irrigation water availability in the Spring. The story was
 568 also highlighted in NASA Earth Observatory March 2018 “Record Low Snowpack in Afghanistan”
 569 (NASA Earth Observatory, 2018).
 570

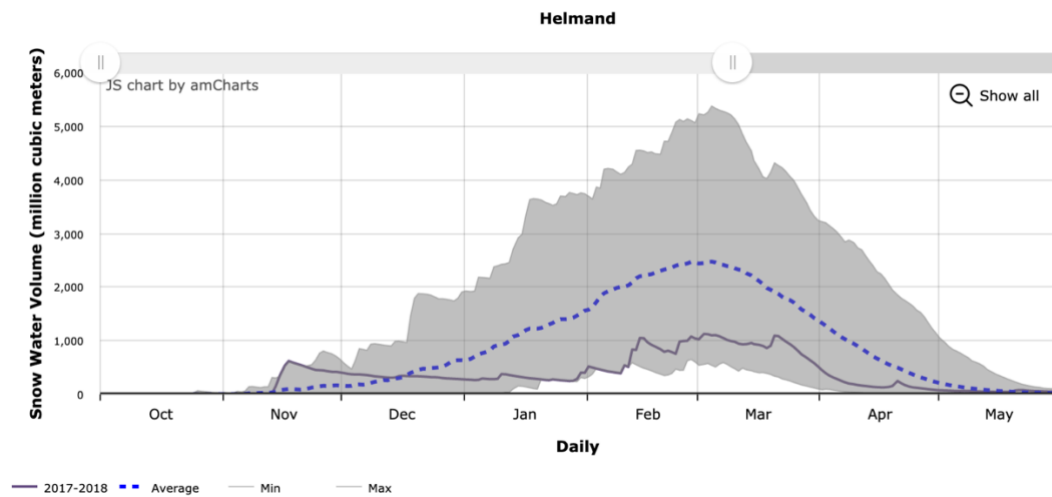
571 The USGS Early Warning eXplorer (EWX) (Shukla et al., 2021) allows analysts to look at maps
572 and time series for a variety of variables and specific provinces and river basins. Plots from EWX in
573 Fig. 10 show below average precipitation for provinces in the Helmand Basin for January and
574 February. CHIRPS cumulative rainfall for 2017-18 versus the 18-year average for Day Kundi (a.k.a.
575 Daykundi) Province showed near average conditions until December. From January, cumulative
576 rainfall remained below the 2000-2018 average throughout the rest of the season ending in May; the
577 same pattern occurred in nearby Uruzgan Province. In neighboring Maydan Wardak (a.k.a Wardak)
578 Province, below average conditions were experienced in January and February, but cumulative
579 rainfall recovered in March to remain slightly above average. Day Kundi (Fig. 10b) and Wardak
580 (Fig. 10c) are provinces located in the upper reaches of the Helmand Basin. Fig. 10c shows SWE
581 averaged across the entire Helmand basin. The gray shading indicates the range of the minimum and
582 maximum values, and the dashed blue line is the average. Initial snow conditions start above
583 average until December, after which SWE deficits are near record low values through the beginning
584 of February, and then persist at below-average levels.



b)



c)



586
587
588
589
590
591
592

Figure 10. (a) CHIRPS cumulative rainfall for 2017-18 versus average conditions for Daykundi Province. (b) CHIRPS cumulative rainfall for 2017-18 versus average conditions for Maydan Wardak Province (c) Helmand Basin SWE from the Central Asia data stream. The grey shading indicates the range of the minimum and maximum values, dashed blue line is the average, and black line is 2017-18. Figures from USGS EWX (<https://earlywarning.usgs.gov/fews/ewx/>).

593 By the end of the season in April 2018, FEWS NET (2018c) concluded that “below-average
594 precipitation throughout most of the country during the October 2017 – May 2018 wet season has
595 led to very low snowpack ...Low irrigation water availability is likely to have an adverse impact on
596 yields for winter wheat and other ...barley, maize, and others.. particularly in downstream areas in
597 regions with limited rainfall. ...The poor performance of the wet season and above average
598 temperatures... exacerbated dry rangeland conditions in many areas, particularly in ...Sari Pul, [and
599 surrounding] ...provinces. Pastoralists and agropastoralists in these areas will likely attempt to
600 migrate to areas with better pasture and water availability or sell livestock at below-average prices.”
601 At the same time, UNICEF (2018) reported in April 2018 that among “the [drought] affected
602 provinces, Baghis, Bamyan, Daykundi, Ghor, Helmand, ... and Uruzgan are of critical priority for
603 nutrition and water, sanitation and hygiene assistance.”
604

605 Several months after a season has ended, and harvest is complete, more statistics become available
606 for further verification of the drought outcomes. The FEWS NET October 2018 Food Security
607 Outlook (2018a) reported that the 2017-18 drought had significant negative impacts on rainfed
608 wheat production and livestock pasture and body conditions across the country. Reporting statistics
609 from the Afghanistan Ministry of Agriculture, Irrigation, and Livestock, the total wheat production
610 for the 2017-18 season was about 20% below average, where irrigated agriculture performed about
611 average. However, rainfed agricultural production was only about 50% of average, most severely
612 affecting households in Badakhshan, Badhis, and Daykundi provinces. In these locations dry
613 conditions, conflict, poor incomes, and depleted assets were expected to continue to face emergency
614 food insecurity through May 2019.

615 **5. Data Availability**

616 The Central Asia data described in this manuscript can be accessed at the NASA GES DISC
617 repository under data doi 10.5067/VQ4CD3Y9YC0R. The data citation is the following:

618
619 Jacob, Jossy and Slinski, Kimberly (NASA/GSFC/HSL) (2021), FLDAS Noah Land Surface Model
620 L4 Central Asia Daily 0.01 x 0.01 degree, Greenbelt, MD, USA, Goddard Earth Sciences Data and
621 Information Services Center (GES DISC) 10.5067/VQ4CD3Y9YC0R
622

623 The global data described in this manuscript can be accessed at the NASA GES DISC repository
624 under data doi 10.5067/5NHC22T9375G. The data citation is the following:

625
626 McNally, Amy. NASA/GSFC/HSL (2018), FLDAS Noah Land Surface Model L4 Global Monthly
627 0.1 x 0.1 degree (MERRA-2 and CHIRPS), Greenbelt, MD, USA, Goddard Earth Sciences Data and
628 Information Services Center (GES DISC), 10.5067/5NHC22T9375G
629

630 Currently the USGS EROS Center provides images from these data:
631 <https://earlywarning.usgs.gov/fews/search/Asia/Central%20Asia>, as well as an interactive data
632 viewer, the USGS EWX (<https://earlywarning.usgs.gov/fews/ewx/>).

633 **6. Code availability**

634 The NASA Land Information System Framework (LISF) is publicly available and an open-source
635 software. The software and technical support are available at <https://github.com/NASA-LIS/LISF>.

636 **7. Conclusion**

637 This paper describes a comprehensive hydrologic analysis system for food security monitoring in
638 Central Asia, with analysis focusing on Afghanistan. While these data are tailored to specific needs,
639 they are also applicable to other climate services and research. Our intent is to provide the reader
640 with information regarding the configuration and specification of both the current global and Central
641 Asia data streams. These data are publicly available and available at near-real time for food security
642 decision support. Note that, as an on-going initiative, FLDAS model version and parameters are
643 routinely updated, and the user should consult the version updates provided by the NASA Goddard
644 Earth Science Data and Information Services Center (GES DISC) data provider and documentation
645 on USGS Early Warning website. For example, efforts are currently underway to upgrade to the
646 Noah-MP (Niu et al., 2011) land surface model, which requires some changes in parameters for
647 snow, glaciers and groundwater. This, and future changes, can be informed by the strengths and
648 weaknesses of the data stream configurations that we have discussed in this paper.

649
650 This paper also provides model-model and model-remote sensing comparisons as well as a review
651 of other research that highlights the challenges of quantitative evaluation of models and remote
652 sensing in this region. A key challenge to hydrologic modeling is the considerable uncertainty in the
653 meteorological forcing available for this region, particularly precipitation. Advancements in remote
654 sensing and modeling should help reduce these uncertainties. In addition, the current land surface
655 modeling reflects natural conditions, i.e., they do not include representation of anthropogenic effects
656 such as human water abstractions (e.g., dams for flood control or irrigation, water diversions,
657 groundwater pumping) or land application of abstracted water (i.e., irrigation). These factors affect
658 estimates of runoff, soil moisture, evapotranspiration, and sensible heat flux (land surface
659 temperatures) in irrigated areas. Therefore, it is important to be aware of the limitations and
660 combine with other products (e.g., NDVI or Actual Evapotranspiration (ETA) in irrigated areas)
661 when exploring water and energy balance. Even with improvements to meteorological forcing and
662 modeling parameterizations, errors will remain. Therefore, the ‘convergence of evidence’ approach
663 is beneficial and would be important when assessing hydro-meteorological hazards and associated
664 risks to food and water security. By making the data publicly available the broader food security and
665 water resources communities will be able to provide insights that can lead to improvements in our

666 understanding of the water and energy balance that can ultimately lead to improvements to food and
667 water security decision support systems.

668

669 **8. Author contribution**

670 JJ runs the code, updates websites, and archives routinely. DS maintains LISF code used in paper,
671 JJ, KA, DS, SP conducted model evaluation AM, KS, CPL, SK contributed to design of evaluation.
672 JR, MB, SP manage the data for USGS distribution. AH, JV provide feedback on data quality and
673 interpretation. AM prepared the manuscript with contributions from all co-authors.

674 **9. Acknowledgements**

675 The authors wish to acknowledge the original version of the Central Asia snow modeling with LIS6
676 performed at NOAA National Operational Hydrologic Remote Sensing Center by Greg Fall and
677 Logan Karsten. USGS work was performed under U.S. Agency for International Development
678 (USAID), Bureau of Humanitarian Assistance (BHA) PAPA AID-FFP-T-17-00003 and USGS
679 contract 140G0119C0001. Any use of trade, firm, or product names is for descriptive purposes only
680 and does not imply endorsement by the U.S. Government. KS, AH, DS, JJ, NASA work was
681 performed under USAID BHA PAPA AID-FFP-T-17-00001. KS, AH acknowledge support from
682 the NASA Harvest Consortium (NASA Applied Sciences Grant No. 80NSSC17K0625). Computing
683 resources have been provided by NASA's Center for Climate Simulation (NCCS). Distribution of
684 data from the Goddard Earth Sciences Data and Information Services Center (GES DISC) is funded
685 by NASA's Science Mission Directorate (SMD). We thank NOAA CPC International Desk for use
686 of figures, and the NASA Land Information System Team for software support and development.
687 The authors also thank the USGS reviewer for comments that improved the quality of the
688 manuscript.

689 **10. References**

690 Arsenault, K. R., Houser, P. R., and De Lannoy, G. J. M.: Evaluation of the MODIS snow cover
691 fraction product: Satellite-based snow cover fraction evaluation., *Hydrol. Process.*, 28, 980–998,
692 <https://doi.org/10.1002/hyp.9636>, 2014.

693 Arsenault, K. R., Kumar, S. V., Geiger, J. V., Wang, S., Kemp, E., Mocko, D. M., Beaudoin, H.
694 K., Getirana, A., Navari, M., Li, B., Jacob, J., Wegiel, J., and Peters-Lidard, C. D.: The Land
695 Surface Data Toolkit (LDT v7.2) - A Data Fusion Environment for Land Data Assimilation
696 Systems, *Geosci. Model Dev.*, 11, <https://doi.org/10.5194/gmd-11-3605-2018>, 2018.

697 Barlage, M., Zeng, X., Wei, H., and Mitchell, K. E.: A global 0.05° maximum albedo dataset of
698 snow-covered land based on MODIS observations: Maximum Albedo of Snow-covered, *Geophys.*
699 *Res. Lett.*, 32, <https://doi.org/10.1029/2005GL022881>, 2005.

- 700 Barlow, M., Wheeler, M., Lyon, B., and Cullen, H.: Modulation of Daily Precipitation over
701 Southwest Asia by the Madden–Julian Oscillation, *Monthly Weather Review*, 133, 3579–3594,
702 <https://doi.org/10.1175/MWR3026.1>, 2005.
- 703 Barlow, M., Zaitchik, B., Paz, S., Black, E., Evans, J., and Hoell, A.: A Review of Drought in the
704 Middle East and Southwest Asia, *Journal of Climate*, 29, 8547–8574, <https://doi.org/10.1175/JCLI->
705 [D-13-00692.1](https://doi.org/10.1175/JCLI-D-13-00692.1), 2016.
- 706 Carroll, M., DiMiceli, C., Wooten, M., Hubbard, A., Sohlberg, R., and Townshend, J.: MOD44W
707 MODIS/Terra Land Water Mask Derived from MODIS and SRTM L3 Global 250m SIN Grid V006
708 [Data set]. NASA EOSDIS Land Processes DAAC., 2017.
- 709 Chen, F., Mitchell, K., Schaake, J., Xue, Y., Pan, H.-L., Koren, V., Duan, Q. Y., Ek, M., and Betts,
710 A.: Modeling of land surface evaporation by four schemes and comparison with FIFE observations,
711 *J. Geophys. Res.*, 101, 7251–7268, <https://doi.org/10.1029/95JD02165>, 1996.
- 712 CIA World Factbook: <https://www.cia.gov/the-world-factbook/countries/afghanistan/#introduction>.
- 713 Cosgrove, B. A., Lohmann, D., Mitchell, K. E., Houser, P. R., Wood, E. F., Schaake, J. C., Robock,
714 A., Marshall, C., Sheffield, J., Duan, Q., Luo, L., Higgins, R. W., Pinker, R. T., Tarpley, J. D., and
715 Meng, J.: Real-time and retrospective forcing in the North American Land Data Assimilation
716 System (NLDAS) project, *J. Geophys. Res.*, 108, 2002JD003118,
717 <https://doi.org/10.1029/2002JD003118>, 2003.
- 718 CPC NOAA: Weather Hazards Outlook of Afghanistan and Central Asia for the Period of February
719 22 - 28, 2018, 2018.
- 720 Csiszar, I. and Gutman, G.: Mapping global land surface albedo from NOAA AVHRR, 104, 6215–
721 6228, <https://doi.org/10.1029/1998JD200090>, 1999.
- 722 Davenport, F. M., Harrison, L., Shukla, S., Husak, G., Funk, C., and McNally, A.: Using out-of-
723 sample yield forecast experiments to evaluate which earth observation products best indicate end of
724 season maize yields, *Environ. Res. Lett.*, 14, 124095, <https://doi.org/10.1088/1748-9326/ab5ccd>,
725 2019.
- 726 Derber, J. C., Parrish, D. F., and Lord, S. J.: The New Global Operational Analysis System at the
727 National Meteorological Center, *Weather and Forecasting*, 6, 538–547,
728 [https://doi.org/10.1175/1520-0434\(1991\)006<0538:TNGOAS>2.0.CO;2](https://doi.org/10.1175/1520-0434(1991)006<0538:TNGOAS>2.0.CO;2), 1991.
- 729 Dezfuli, A. K., Ichoku, C. M., Huffman, G. J., Mohr, K. I., Selker, J. S., van de Giesen, N.,
730 Hochreutener, R., and Annor, F. O.: Validation of IMERG Precipitation in Africa, *Journal of*
731 *Hydrometeorology*, 18, 2817–2825, <https://doi.org/10.1175/JHM-D-17-0139.1>, 2017.

- 732 Ek, M. B., Mitchell, K. E., Lin, Y., Rogers, E., Grunmann, P., Koren, V., Gayno, G., and Tarpley, J.
733 D.: Implementation of Noah land surface model advances in the National Centers for Environmental
734 Prediction operational mesoscale Eta model, *JGR: Atmospheres*, 108,
735 <https://doi.org/10.1029/2002JD003296>, 2003.
- 736 Ellenburg, W. L., Mishra, V., Roberts, J. B., Limaye, A. S., Case, J. L., Blankenship, C. B., and
737 Cressman, K.: Detecting Desert Locust Breeding Grounds: A Satellite-Assisted Modeling
738 Approach, *Remote Sensing*, 13, 1276, <https://doi.org/10.3390/rs13071276>, 2021.
- 739 Entekhabi, D., Njoku, E. G., O'Neill, P. E., Kellogg, K. H., Crow, W. T., Edelstein, W. N., Entin, J.
740 K., Goodman, S. D., Jackson, T. J., Johnson, J., Kimball, J., Piepmeier, J. R., Koster, R. D., Martin,
741 N., McDonald, K. C., Moghaddam, M., Moran, S., Reichle, R., Shi, J. C., Spencer, M. W.,
742 Thurman, S. W., Tsang, L., and Zyl, J. V.: The Soil Moisture Active Passive (SMAP) Mission, 98,
743 704–716, <https://doi.org/10.1109/JPROC.2010.2043918>, 2010.
- 744 Entekhabi, D., Das, N., Njoku, E. G., Johnson, J., and Shi, J. C.: SMAP L3 Radar/Radiometer
745 Global Daily 9 km EASE-Grid Soil Moisture, Version 3, NASA National Snow and Ice Data Center
746 DAAC [preprint], <https://doi.org/10.5067/7KKNQ5UURM2W>, 2016.
- 747 FEWS NET: Afghanistan Food Security Outlook October 2017-May 2018 Conflict, dry spells, and
748 weak labor opportunities will lead to deterioration in outcomes during 2018 lean season, 2017a.
- 749 FEWS NET: Update on performance of the October 2016 – May 2017 wet season, 2017b.
- 750 FEWS NET: Afghanistan Food Security Outlook: Emergency assistance needs are atypically high
751 through the lean season across the country, FEWS NET, 2018a.
- 752 FEWS NET: Afghanistan Food Security Outlook February to September 2018: Low snow
753 accumulation and dry soil conditions likely to impact 2018 staple production, 2018b.
- 754 FEWS NET: Afghanistan Food Security Outlook Update April 2018: Poor rangeland conditions and
755 below-average water availability will limit seasonal improvements, 2018c.
- 756 FEWS NET: El Niño and Precipitation, FEWS NET, [https://fews.net/el-ni%C3%B1o-and-](https://fews.net/el-ni%C3%B1o-and-precipitation)
757 [precipitation](https://fews.net/el-ni%C3%B1o-and-precipitation), 2020a.
- 758 FEWS NET: La Niña and Precipitation, FEWS NET, [https://fews.net/la-ni%C3%B1a-and-](https://fews.net/la-ni%C3%B1a-and-precipitation)
759 [precipitation](https://fews.net/la-ni%C3%B1a-and-precipitation), 2020b.
- 760 FEWS NET: Afghanistan Food Security Outlook February to September 2021: Below-average
761 precipitation likely to drive below-average agricultural and livestock production in 2021, 2021.

762 Funk, C., Peterson, P., Landsfeld, M., Pedreros, D., Verdin, J., Shukla, S., Husak, G., Rowland, J.,
763 Harrison, L., Hoell, A., and Michaelsen, J.: The climate hazards infrared precipitation with stations--
764 a new environmental record for monitoring extremes., The climate hazards infrared precipitation
765 with stations—a new environmental record for monitoring extremes, *Sci Data*, 2, 2, 150066–
766 150066, <https://doi.org/10.1038/sdata.2015.66>, 10.1038/sdata.2015.66, 2015.

767 Funk, C. C., Peterson, P., Huffman, G. J., Landsfeld, M. F., Peters-Lidard, C., Davenport, F.,
768 Shukla, S., Peterson, S., Pedreros, D. H., Ruane, A. C., Mutter, C., Turner, W., Harrison, L.,
769 Sonnier, A., Way-Henthorne, J., and Husak, G. J.: Introducing and Evaluating the Climate Hazards
770 Center IMERG with Stations (CHIMES): Timely Station-Enhanced Integrated Multisatellite
771 Retrievals for Global Precipitation Measurement, 103, E429–E454, [https://doi.org/10.1175/BAMS-](https://doi.org/10.1175/BAMS-D-20-0245.1)
772 [D-20-0245.1](https://doi.org/10.1175/BAMS-D-20-0245.1), 2022.

773 Gadelha, A. N., Coelho, V. H. R., Xavier, A. C., Barbosa, L. R., Melo, D. C. D., Xuan, Y.,
774 Huffman, G. J., Petersen, W. A., and Almeida, C. das N.: Grid box-level evaluation of IMERG over
775 Brazil at various space and time scales, *Atmospheric Research*, 218, 231–244,
776 <https://doi.org/10.1016/j.atmosres.2018.12.001>, 2019.

777 Gelaro, R., McCarty, W., Suárez, M. J., Todling, R., Molod, A., Takacs, L., Randles, C. A.,
778 Darmenov, A., Bosilovich, M. G., Reichle, R., Wargan, K., Coy, L., Cullather, R., Draper, C.,
779 Akella, S., Buchard, V., Conaty, A., da Silva, A. M., Gu, W., Kim, G.-K., Koster, R., Lucchesi, R.,
780 Merkova, D., Nielsen, J. E., Partyka, G., Pawson, S., Putman, W., Rienecker, M., Schubert, S. D.,
781 Sienkiewicz, M., and Zhao, B.: The Modern-Era Retrospective Analysis for Research and
782 Applications, Version 2 (MERRA-2), *J. Climate*, 30, 5419–5454, [https://doi.org/10.1175/JCLI-D-](https://doi.org/10.1175/JCLI-D-16-0758.1)
783 [16-0758.1](https://doi.org/10.1175/JCLI-D-16-0758.1), 2017.

784 GEOGLAM: Early Warning Crop Monitor February 2018,
785 https://cropmonitor.org/documents/EWCM/reports/EarlyWarning_CropMonitor_201802.pdf,
786 2018a.

787 GEOGLAM: Early Warning Crop Monitor March 2018,
788 https://cropmonitor.org/documents/EWCM/reports/EarlyWarning_CropMonitor_201802.pdf,
789 2018b.

790 Ghatak, D., Zaitchik, B., Kumar, S., Matin, M. A., Bajracharya, B., Hain, C., and Anderson, M.:
791 Influence of Precipitation Forcing Uncertainty on Hydrological Simulations with the NASA South
792 Asia Land Data Assimilation System, *Hydrology*, 5, 57, <https://doi.org/10.3390/hydrology5040057>,
793 2018.

794 Grace, K. and Davenport, F.: Climate variability and health in extremely vulnerable communities:
795 investigating variations in surface water conditions and food security in the West African Sahel,
796 *Population & Environment*, 42, 553–577, <https://doi.org/10.1007/s11111-021-00375-9>, 2021.

- 797 Gutman, G. and Ignatov, A.: The derivation of the green vegetation fraction from NOAA/AVHRR
798 data for use in numerical weather prediction models, *International Journal of Remote Sensing*, 19,
799 1533–1543, <https://doi.org/10.1080/014311698215333>, 1998.
- 800 Hall, D. and Riggs, G.: MODIS/Terra Snow Cover Daily L3 Global 500m SIN Grid version 6,
801 <https://doi.org/10.5067/MODIS/MOD10A1.006>, 2016.
- 802 Hengl, T., Jesus, J. M. de, Heuvelink, G. B. M., Gonzalez, M. R., Kilibarda, M., Blagotić, A.,
803 Shangguan, W., Wright, M. N., Geng, X., Bauer-Marschallinger, B., Guevara, M. A., Vargas, R.,
804 MacMillan, R. A., Batjes, N. H., Leenaars, J. G. B., Ribeiro, E., Wheeler, I., Mantel, S., and
805 Kempen, B.: SoilGrids250m: Global gridded soil information based on machine learning, *PLOS*
806 *ONE*, 12, e0169748, <https://doi.org/10.1371/journal.pone.0169748>, 2017.
- 807 Hewitt, C., Mason, S., and Walland, D.: The Global Framework for Climate Services, *Nature Clim*
808 *Change*, 2, 831–832, <https://doi.org/10.1038/nclimate1745>, 2012.
- 809 Hoell, A., Funk, C., and Barlow, M.: The Forcing of Southwestern Asia Teleconnections by Low-
810 Frequency Sea Surface Temperature Variability during Boreal Winter, *J. Climate*, 28, 1511–1526,
811 <https://doi.org/10.1175/JCLI-D-14-00344.1>, 2015.
- 812 Hoell, A., Barlow, M., Cannon, F., and Xu, T.: Oceanic Origins of Historical Southwest Asia
813 Precipitation During the Boreal Cold Season, *J. Climate*, 30, 2885–2903,
814 <https://doi.org/10.1175/JCLI-D-16-0519.1>, 2017.
- 815 Hoell, A., Cannon, F., and Barlow, M.: Middle East and Southwest Asia Daily Precipitation
816 Characteristics Associated with the Madden–Julian Oscillation during Boreal Winter, *J. Climate*, 31,
817 8843–8860, <https://doi.org/10.1175/JCLI-D-18-0059.1>, 2018.
- 818 Hoell, A., Eischeid, J., Barlow, M., and McNally, A.: Characteristics, precursors, and potential
819 predictability of Amu Darya Drought in an Earth system model large ensemble, *Clim Dyn*, 55,
820 2185–2206, <https://doi.org/10.1007/s00382-020-05381-5>, 2020.
- 821 Huffman, G. J., Bolvin, D. T., Braithwaite, D., Hsu, K.-L., Joyce, R. J., Kidd, C., Nelkin, E. J.,
822 Sorooshian, S., Stocker, E. F., Tan, J., Wolff, D. B., and Xie, P.: Integrated Multi-satellite Retrievals
823 for the Global Precipitation Measurement (GPM) Mission (IMERG), in: *Satellite Precipitation*
824 *Measurement: Volume 1*, edited by: Levizzani, V., Kidd, C., Kirschbaum, D. B., Kummerow, C. D.,
825 Nakamura, K., and Turk, F. J., Springer International Publishing, Cham, 343–353,
826 https://doi.org/10.1007/978-3-030-24568-9_19, 2020.
- 827 Immerzeel, W. W., Wanders, N., Lutz, A. F., Shea, J. M., and Bierkens, M. F. P.: Reconciling high-
828 altitude precipitation in the upper Indus basin with glacier mass balances and runoff, *Hydrol. Earth*
829 *Syst. Sci.*, 19, 4673–4687, <https://doi.org/10.5194/hess-19-4673-2015>, 2015.

- 830 Jacob, J. and Slinski, K.: GES DISC Dataset: FLDAS Noah Land Surface Model L4 Central Asia
831 Daily 0.01 x 0.01 degree (FLDAS_NOAH001_G_CA_D 001),
832 <https://doi.org/10.5067/VQ4CD3Y9YC0R>, 2021.
- 833 Jung, H. C., Getirana, A., Policelli, F., McNally, A., Arsenault, K. R., Kumar, S., Tadesse, T., and
834 Peters-Lidard, C. D.: Upper Blue Nile basin water budget from a multi-model perspective, *Journal*
835 *of Hydrology*, 555, 535–546, <https://doi.org/10.1016/j.jhydrol.2017.10.040>, 2017.
- 836 Jung, H. C., Getirana, A., Arsenault, K. R., Holmes, T. R. H., and McNally, A.: Uncertainties in
837 Evapotranspiration Estimates over West Africa, *Remote Sensing*, 11, 892,
838 <https://doi.org/10.3390/rs11080892>, 2019.
- 839 Kato, H. and Rodell, M.: Sensitivity of Land Surface Simulations to Model Physics, Land
840 Characteristics, and Forcings, at Four CEOP Sites, *Journal of the Meteorological Society of Japan*.
841 Ser. II, Volume 85A, 187–204, <https://doi.org/10.2151/jmsj.85A.187>, 2007.
- 842 Kirschbaum, D. B., Huffman, G. J., Adler, R. F., Braun, S., Garrett, K., Jones, E., McNally, A.,
843 Skofronick-Jackson, G., Stocker, E., Wu, H., and Zaitchik, B. F.: NASA's Remotely Sensed
844 Precipitation: A Reservoir for Applications Users, *Bull. Amer. Meteor. Soc.*, 98, 1169–1184,
845 <https://doi.org/10.1175/BAMS-D-15-00296.1>, 2016.
- 846 Kumar, S. V., Peters-Lidard, C. D., Tian, Y., Houser, P. R., Geiger, J., Olden, S., Lighty, L.,
847 Eastman, J. L., Doty, B., Dirmeyer, P., Adams, J., Mitchell, K., Wood, E. F., and Sheffield, J.: Land
848 information system: An interoperable framework for high resolution land surface modeling,
849 *Environmental Modelling & Software*, 21, 1402–1415,
850 <https://doi.org/10.1016/j.envsoft.2005.07.004>, 2006.
- 851 Kumar, S. V., Peters-Lidard, C. D., Santanello, J., Harrison, K., Liu, Y., and Shaw, M.: Land
852 surface Verification Toolkit (LVT) – a generalized framework for land surface model evaluation,
853 *Geosci. Model Dev.*, 5, 869–886, <https://doi.org/10.5194/gmd-5-869-2012>, 2012.
- 854 Kumar, S. V., Peters-Lidard, C. D., Mocko, D., and Tian, Y.: Multiscale Evaluation of the
855 Improvements in Surface Snow Simulation through Terrain Adjustments to Radiation, *Journal of*
856 *Hydrometeorology*, 14, 220–232, <https://doi.org/10.1175/JHM-D-12-046.1>, 2013.
- 857 Ma, Z., Xu, J., Zhu, S., Yang, J., Tang, G., Yang, Y., Shi, Z., and Hong, Y.: AIMERG: a new Asian
858 precipitation dataset (0.1°/half-hourly, 2000–2015) by calibrating the GPM-era IMERG at a daily
859 scale using APHRODITE, *Earth Syst. Sci. Data*, 12, 1525–1544, [https://doi.org/10.5194/essd-12-](https://doi.org/10.5194/essd-12-1525-2020)
860 [1525-2020](https://doi.org/10.5194/essd-12-1525-2020), 2020.
- 861 Manz, B., Páez-Bimos, S., Horna, N., Buytaert, W., Ochoa-Tocachi, B., Lavado-Casimiro, W., and
862 Willems, B.: Comparative Ground Validation of IMERG and TMPA at Variable Spatiotemporal

- 863 Scales in the Tropical Andes, *Journal of Hydrometeorology*, 18, 2469–2489,
864 <https://doi.org/10.1175/JHM-D-16-0277.1>, 2017.
- 865 McNally, A.: GES DISC Dataset: FLDAS Noah Land Surface Model L4 Global Monthly 0.1 x 0.1
866 degree (MERRA-2 and CHIRPS) (FLDAS_NOAH01_C_GL_M 001), 2018.
- 867 McNally, A., Husak, G. J., Brown, M., Carroll, M., Funk, C., Yatheendradas, S., Arsenault, K.,
868 Peters-Lidard, C., and Verdin, J. P.: Calculating Crop Water Requirement Satisfaction in the West
869 Africa Sahel with Remotely Sensed Soil Moisture, *J. Hydrometeor.*, 16, 295–305,
870 <https://doi.org/10.1175/JHM-D-14-0049.1>, 2015.
- 871 McNally, A., Shukla, S., Arsenault, K. R., Wang, S., Peters-Lidard, C. D., and Verdin, J. P.:
872 Evaluating ESA CCI soil moisture in East Africa, *International Journal of Applied Earth
873 Observation and Geoinformation*, 48, 96–109, <https://doi.org/10.1016/j.jag.2016.01.001>, 2016.
- 874 McNally, A., Arsenault, K., Kumar, S., Shukla, S., Peterson, P., Wang, S., Funk, C., Peters-lidard,
875 C. D., and Verdin, J. P.: A land data assimilation system for sub-Saharan Africa food and water
876 security applications, *Scientific Data*, 4, 170012, <http://dx.doi.org/10.1038/sdata.2017.12>, 2017.
- 877 McNally, A., McCartney, S., Ruane, A. C., Mladenova, I. E., Whitcraft, A. K., Becker-Reshef, I.,
878 Bolten, J. D., Peters-Lidard, C. D., Rosenzweig, C., and Uz, S. S.: Hydrologic and Agricultural
879 Earth Observations and Modeling for the Water-Food Nexus, *Front. Environ. Sci.*, 7,
880 <https://doi.org/10.3389/fenvs.2019.00023>, 2019.
- 881 Miller, J., Barlage, M., Zeng, X., Wei, H., Mitchell, K., and Tarpley, D.: Sensitivity of the
882 NCEP/Noah land surface model to the MODIS green vegetation fraction data set, *Geophys. Res.
883 Lett.*, 33, <https://doi.org/10.1029/2006GL026636>, 2006.
- 884 Molteni, F., Buizza, R., Palmer, T. N., and Petroliagis, T.: The ECMWF Ensemble Prediction
885 System: Methodology and validation, *Q J R Meteorol Soc*, 122, 73–119,
886 <https://doi.org/10.1002/qj.49712252905>, 1996.
- 887 NASA Earth Observatory: Record Low Snowpack in Afghanistan, NASA Earth Observatory, 2018.
- 888 NASA JPL: NASA Shuttle Radar Topography Mission Global 30 arc second [Data set]. NASA
889 EOSDIS Land Processes DAAC, NASA EOSDIS Land Processes DAAC, NASA EOSDIS Land
890 Processes DAAC., 2013.
- 891 Nazemosadat, M. J. and Ghaedamini, H.: On the Relationships between the Madden–Julian
892 Oscillation and Precipitation Variability in Southern Iran and the Arabian Peninsula: Atmospheric
893 Circulation Analysis, 23, 887–904, <https://doi.org/10.1175/2009JCLI2141.1>, 2010.

- 894 NCAR Research Applications Library: <https://ral.ucar.edu/solutions/products/unified-noah-lsm>, last
895 access: 12 November 2021.
- 896 Niu, G.-Y., Yang, Z.-L., Mitchell, K. E., Chen, F., Ek, M. B., Barlage, M., Kumar, A., Manning, K.,
897 Niyogi, D., Rosero, E., Tewari, M., and Xia, Y.: The community Noah land surface model with
898 multiparameterization options (Noah-MP): 1. Model description and evaluation with local-scale
899 measurements, *JGR: Atmospheres*, 116, <https://doi.org/10.1029/2010JD015139>, 2011.
- 900 NOAA: [https://www.climate.gov/news-features/blogs/enso/september-enso-update-la-ni%C3%B1a-](https://www.climate.gov/news-features/blogs/enso/september-enso-update-la-ni%C3%B1a-watch)
901 [watch](https://www.climate.gov/news-features/blogs/enso/september-enso-update-la-ni%C3%B1a-watch), last access: 12 September 2017.
- 902 NOAA CPC ENSO Cold & Warm Episodes by Season:
903 https://origin.cpc.ncep.noaa.gov/products/analysis_monitoring/ensostuff/ONI_v5.php, last access:
904 29 July 2021.
- 905 Oki, T. and Kanae, S.: Global Hydrological Cycles and World Water Resources, *Science*, 313,
906 1068–1072, <https://doi.org/10.1126/science.1128845>, 2006.
- 907 Pervez, S., McNally, A., Arsenault, K., Budde, M., and Rowland, J.: Vegetation Monitoring
908 Optimization With Normalized Difference Vegetation Index and Evapotranspiration Using Remote
909 Sensing Measurements and Land Surface Models Over East Africa, *Frontiers in Climate*, 3, 1,
910 <https://doi.org/10.3389/fclim.2021.589981>, 2021.
- 911 Peters-Lidard, C. D., Houser, P. R., Tian, Y., Kumar, S. V., Geiger, J., Olden, S., Lighty, L., Doty,
912 B., Dirmeyer, P., Adams, J., Mitchell, K., Wood, E. F., and Sheffield, J.: High-performance Earth
913 system modeling with NASA/GSFC’s Land Information System, *Innovations Syst Softw Eng*, 3,
914 157–165, <https://doi.org/10.1007/s11334-007-0028-x>, 2007.
- 915 Qamer, F. M., Tadesse, T., Matin, M., Ellenburg, W. L., and Zaitchik, B.: Earth Observation and
916 Climate Services for Food Security and Agricultural Decision Making in South and Southeast Asia,
917 *Bull Am Meteorol Soc*, 100, ES171–ES174, <https://doi.org/10.1175/BAMS-D-18-0342.1>, 2019.
- 918 Rana, S., Renwick, J., McGregor, J., and Singh, A.: Seasonal Prediction of Winter Precipitation
919 Anomalies over Central Southwest Asia: A Canonical Correlation Analysis Approach, *J. Climate*,
920 31, 727–741, <https://doi.org/10.1175/JCLI-D-17-0131.1>, 2018.
- 921 Reynolds, C. A., Jackson, T. J., and Rawls, W. J.: Estimating soil water-holding capacities by
922 linking the Food and Agriculture Organization Soil map of the world with global pedon databases
923 and continuous pedotransfer functions, *Water Resources Research*, 36, 3653–3662,
924 <https://doi.org/10.1029/2000WR900130>, 2000.

- 925 Sarmiento, D. P., Slinski, K., McNally, A., Funk, C., Peterson, P., and Peters-Lidard, C. D.: Daily
926 precipitation frequency distributions impacts on land-surface simulations of CONUS, *Front. Water*,
927 0, <https://doi.org/10.3389/frwa.2021.640736>, 2021.
- 928 Schiemann, R., Lüthi, D., Vidale, P. L., and Schär, C.: The precipitation climate of Central Asia—
929 intercomparison of observational and numerical data sources in a remote semiarid region, *Royal*
930 *Meteorological Society*, 28, 295–314, <https://doi.org/10.1002/joc.1532>, 2008.
- 931 Schneider, U., Finger, P., Meyer-Christoffer, A., Rustemeier, E., Ziese, M., and Becker, A.:
932 Evaluating the Hydrological Cycle over Land Using the Newly-Corrected Precipitation Climatology
933 from the Global Precipitation Climatology Centre (GPCC), 8, 52,
934 <https://doi.org/10.3390/atmos8030052>, 2017.
- 935 Senay, G. B., Bohms, S., Singh, R. K., Gowda, P. H., Velpuri, N. M., Alemu, H., and Verdin, J. P.:
936 Operational Evapotranspiration Mapping Using Remote Sensing and Weather Datasets: A New
937 Parameterization for the SSEB Approach, *J Am Water Resour Assoc*, 49, 577–591,
938 <https://doi.org/10.1111/jawr.12057>, 2013.
- 939 Shukla, S., Arsenault, K. R., Hazra, A., Peters-Lidard, C., Koster, R. D., Davenport, F., Magadzire,
940 T., Funk, C., Kumar, S., McNally, A., Getirana, A., Husak, G., Zaitchik, B., Verdin, J., Nsadisa, F.
941 D., and Becker-Reshef, I.: Improving early warning of drought-driven food insecurity in southern
942 Africa using operational hydrological monitoring and forecasting products, *Nat. Hazards Earth Syst.*
943 *Sci.*, 20, 1187–1201, <https://doi.org/10.5194/nhess-20-1187-2020>, 2020.
- 944 Shukla, S., Landsfeld, M., Anthony, M., Budde, M., Husak, G. J., Rowland, J., and Funk, C.:
945 Enhancing the Application of Earth Observations for Improved Environmental Decision-Making
946 Using the Early Warning eXplorer (EWX), *Frontiers in Climate*, 2, 34,
947 <https://doi.org/10.3389/fclim.2020.583509>, 2021.
- 948 Tabar, M., Gluck, J., Goyal, A., Jiang, F., Morr, D., Kehs, A., Lee, D., Hughes, D. P., and Yadav,
949 A.: A PLAN for Tackling the Locust Crisis in East Africa: Harnessing Spatiotemporal Deep Models
950 for Locust Movement Forecasting, in: *Proceedings of the 27th ACM SIGKDD Conference on*
951 *Knowledge Discovery & Data Mining*, New York, NY, USA, 3595–3604,
952 <https://doi.org/10.1145/3447548.3467184>, 2021.
- 953 Tan, J., Petersen, W. A., and Tokay, A.: A Novel Approach to Identify Sources of Errors in IMERG
954 for GPM Ground Validation, *Journal of Hydrometeorology*, 17, 2477–2491,
955 <https://doi.org/10.1175/JHM-D-16-0079.1>, 2016.
- 956 UNICEF: 500,000 children affected by drought in Afghanistan – UNICEF,
957 <https://www.unicef.org/press-releases/500000-children-affected-drought-afghanistan-unicef>, 2018.

- 958 USGS Knowledge Base:
959 <https://earlywarning.usgs.gov/fews/searchkb/Asia/Central%20Asia/Afghanistan>, last access: 12
960 November 2021.
- 961 Vincent, K., Daly, M., Scannell, C., and Leathes, B.: What can climate services learn from theory
962 and practice of co-production?, *Climate Services*, 12, 48–58,
963 <https://doi.org/10.1016/j.cliser.2018.11.001>, 2018.
- 964 Xie, P. and Arkin, P. A.: Analyses of Global Monthly Precipitation Using Gauge Observations,
965 Satellite Estimates, and Numerical Model Predictions, *Journal of Climate*, 9, 840–858,
966 [https://doi.org/10.1175/1520-0442\(1996\)009<0840:AOGMPU>2.0.CO;2](https://doi.org/10.1175/1520-0442(1996)009<0840:AOGMPU>2.0.CO;2), 1996.
- 967 Yatagai, A., Kamiguchi, K., Arakawa, O., Hamada, A., Yasutomi, N., and Kito, A.: APHRODITE:
968 Constructing a Long-Term Daily Gridded Precipitation Dataset for Asia Based on a Dense Network
969 of Rain Gauges, *Bull Am Meteorol Soc*, 93, 1401–1415, [https://doi.org/10.1175/BAMS-D-11-](https://doi.org/10.1175/BAMS-D-11-00122.1)
970 [00122.1](https://doi.org/10.1175/BAMS-D-11-00122.1), 2012.
- 971 Yoon, Y., Kumar, S. V., Forman, B. A., Zaitchik, B. F., Kwon, Y., Qian, Y., Rupper, S., Maggioni,
972 V., Houser, P., Kirschbaum, D., Richey, A., Arendt, A., Mocko, D., Jacob, J., Bhanja, S., and
973 Mukherjee, A.: Evaluating the Uncertainty of Terrestrial Water Budget Components Over High
974 Mountain Asia, *Frontiers in Earth Science*, 7, 120, <https://doi.org/10.3389/feart.2019.00120>, 2019.

975